

Caenorhabditis elegans transthyretin-like protein TTR-52 mediates recognition of apoptotic cells by the CED-1 phagocyte receptor

Xiaochen Wang^{1,2,5}, Weida Li^{2,4}, Dongfeng Zhao^{2,4}, Bin Liu^{2,4}, Yong Shi^{1,4}, Baohui Chen², Hengwen Yang¹, Pengfei Guo², Xin Geng¹, Zhihong Shang¹, Erin Peden¹, Eriko Kage-Nakadai³, Shohei Mitani³ and Ding Xue^{1,5}

During apoptosis, dying cells are swiftly removed by phagocytes. It is not fully understood how apoptotic cells are recognized by phagocytes. Here we report the identification and characterization of the *Caenorhabditis elegans* *ttr-52* gene, which encodes a transthyretin-like protein and is required for efficient cell corpse engulfment. The TTR-52 protein is expressed in, and secreted from, *C. elegans* endoderm and clusters around apoptotic cells. Genetic analysis indicates that TTR-52 acts in the cell corpse engulfment pathway mediated by CED-1, CED-6 and CED-7 and affects clustering of the phagocyte receptor CED-1 around apoptotic cells. TTR-52 recognizes surface-exposed phosphatidylserine (PtdSer) *in vivo* and binds to both PtdSer and the extracellular domain of CED-1 *in vitro*. TTR-52 is therefore the first bridging molecule identified in *C. elegans* that mediates recognition of apoptotic cells by crosslinking the PtdSer 'eat me' signal with the phagocyte receptor CED-1.

The phagocytosis and removal of apoptotic cells is an important event in tissue remodelling, suppression of inflammation and regulation of immune responses^{1,2}. During apoptosis, apoptotic cells expose various 'eat-me' signals, which are recognized by phagocytes either directly through phagocyte receptors or indirectly through bridging molecules that crosslink apoptotic cells to phagocytes³. The recognition of 'eat-me' signals by phagocytes triggers signalling cascades, leading to the internalization and degradation of apoptotic cells by phagocytes³.

In *C. elegans*, phagocytosis of apoptotic cells is controlled by two partly redundant signalling pathways⁴. In one pathway, several conserved intracellular signalling molecules, namely CED-2/CrkII, CED-5/DOCK180 and CED-12/ELMO, mediate the activation of the small GTPase CED-10/Rac1, leading to the cytoskeleton reorganization needed for phagocytosis^{5–9}. In the other pathway, three genes, namely *ced-1*, *ced-6* and *ced-7*, are involved in recognizing and transducing 'eat-me' signals. *ced-1* encodes a single-pass transmembrane protein that acts in engulfing cells to promote removal of apoptotic cells¹⁰. The CED-1–GFP (green fluorescent protein) fusion is found to cluster specifically around apoptotic cells¹⁰, indicating that CED-1 has a function in recognizing apoptotic cells. CED-1 shares sequence similarity with several mammalian cell-surface proteins, including Scavenger Receptor from Endothelial Cells, LRP/CD91 and MEGF10 (multiple EGF-like-domains 10), and two *Drosophila* proteins, Draper

and Six-microns-under (SIMU), all of which have been implicated in the phagocytosis of apoptotic cells^{10–15}. Some, like CED-1, are involved in the recognition of apoptotic cells^{14,16}. MEGF10 can partly substitute for the function of CED-1 in *C. elegans*¹². CED-1 therefore defines a conserved family of phagocyte receptors that are important in the recognition and removal of apoptotic cells.

It is not clear how CED-1 family proteins recognize apoptotic cells. One potential signal recognized by CED-1 is PtdSer exposed on the surface of apoptotic cells, which has been shown to be a conserved 'eat-me' signal^{17,18}. Indeed, PtdSer is detected on the surface of most *C. elegans* apoptotic cells and has been found to be important for cell corpse engulfment^{19–22}. In animals lacking TAT-1, an aminophospholipid translocase that maintains plasma membrane PtdSer asymmetry, PtdSer is ectopically exposed on the surface of normal cells, which triggers the removal of normal cells in a CED-1-dependent manner²². CED-1 may therefore recognize, and mediate the removal of, cells with surface-exposed PtdSer. However, CED-1 or its homologues are not known to bind PtdSer directly and may recognize PtdSer through an intermediate molecule.

Here we report the identification of a secreted protein, TTR-52, that binds surface-exposed PtdSer on the apoptotic cell and the CED-1 receptor and acts as a bridging molecule to mediate the recognition and engulfment of apoptotic cells by the CED-1-bearing phagocytes.

¹Department of Molecular, Cellular, and Developmental Biology, University of Colorado, Boulder, Co 80309, USA. ²National Institute of Biological Sciences, No. 7 Sciences Park Road, Zhongguancun Life Sciences Park, Beijing, 102206, China. ³Department of Physiology, Tokyo Women's Medical University, School of Medicine, and CREST, JST, 8-1, Kawada-cho, Shinjuku-ku, Tokyo, 162-8666, Japan.

⁴These authors contributed equally to this work.

⁵Correspondence should be addressed to D.X. or X.C.W. (e-mail: ding.xue@colorado.edu; wangxiaochen@nibs.ac.cn)

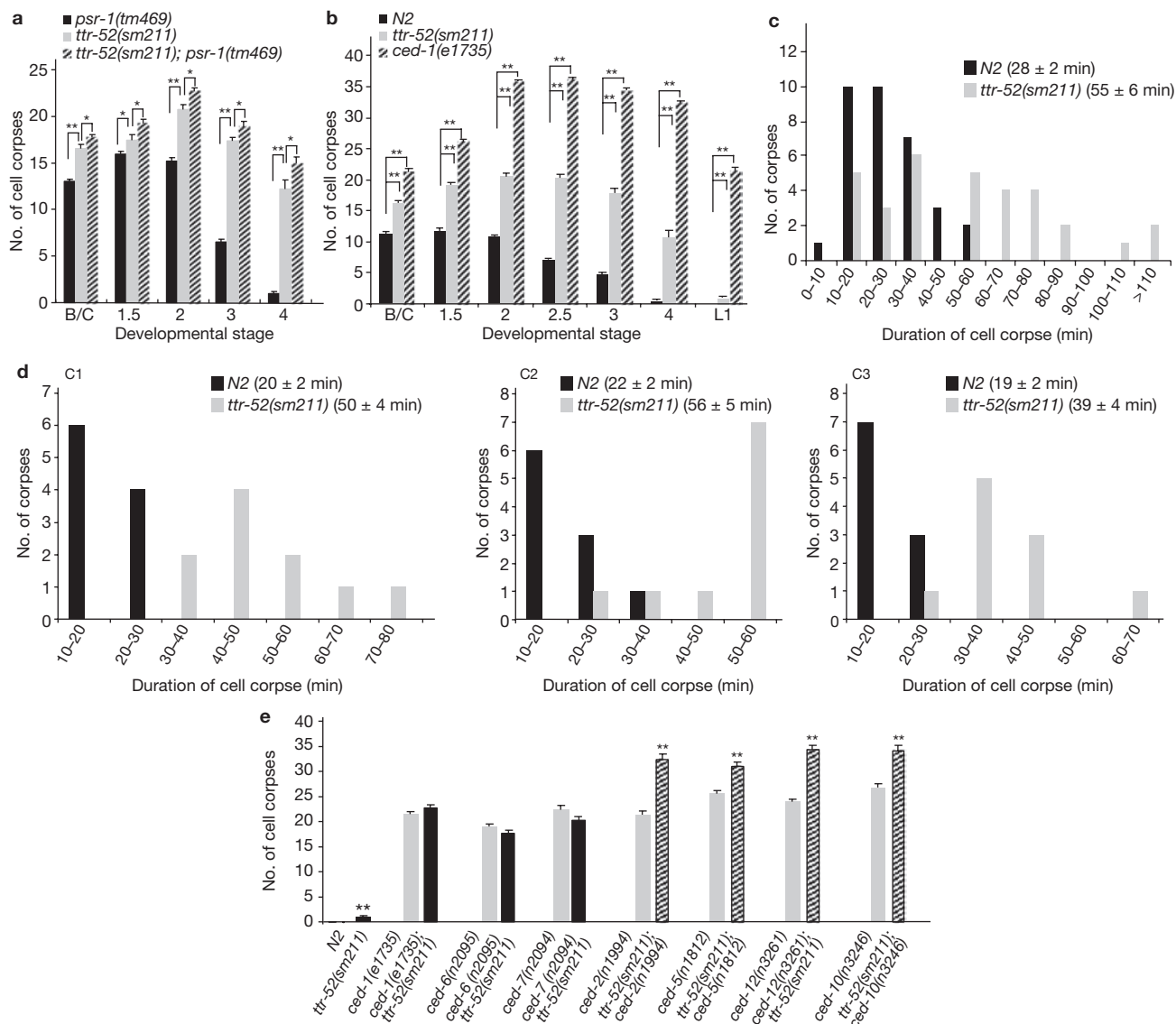


Figure 1 *ttr-52* is important for cell corpse engulfment in *C. elegans*. (a, b) Time-course analysis of cell corpses during development. (a) The *ttr-52(sm211); psr-1(tm469)* double mutant displays a stronger engulfment defect than the single mutants. (b) Comparison of the engulfment defects of the *ttr-52* and *ced-1* mutants. Cell corpses from the indicated strains were scored at six embryonic stages (bean/comma (B/C), 1.5-fold, 2-fold, 2.5-fold, 3-fold, 4-fold) and the early L1 larval stage (L1). The y axis represents the mean number of cell corpses scored at the head region of embryos or L1 larvae (15 animals at each stage). Error bars represent s.e.m. Two asterisks, $P < 0.0001$, asterisk, $P < 0.05$ (see Methods). (c) Four-dimensional microscopy analysis of cell corpse durations in the *ttr-52(sm211)* mutant.

RESULTS

A new mutant defective in cell corpse engulfment

In a genetic screen for mutations that enhance the weak engulfment defect of the *psr-1(tm469)* mutant (see Methods), which lacks the PtdSer-recognizing PSR-1 receptor²³, we isolated a recessive mutation (*sm211*) that not only enhances the *psr-1* engulfment defect but also results in increased cell corpses on its own (Fig. 1a, b). In fact, the numbers of cell corpses observed in the *sm211* mutant at all embryonic stages and the L1 larval stage are significantly higher than those of the wild-type or *psr-1(tm469)* animals (Fig. 1a, b).

The durations of 33 cell corpses from wild-type (*N2*) embryos ($n = 3$, black bars) and 32 cell corpses from *ttr-52(sm211)* embryos ($n = 3$, grey bars) were monitored. The numbers in parentheses indicate the durations of cell corpses (means and s.e.m.). The y axis indicates the number of cell corpses within a specific duration range as shown on the x axis. (d) Corpse durations of C1, C2 and C3 cells were monitored as described in c. Ten corpses each in wild-type and *ttr-52(sm211)* embryos were followed for each cell. (e) *ttr-52(sm211)* enhances the engulfment defect of the *ced-2*, *ced-5*, *ced-10* and *ced-12* mutants. Cell corpses from the indicated strains were scored at the head region of early L1 larvae (15 animals each). Error bars represent s.e.m. Two asterisks, $P < 0.0001$; all other points had $P > 0.05$.

To determine whether *sm211* animals are defective in cell corpse engulfment, we performed a time-lapse analysis to measure the durations of persistence of cell corpses in wild-type and *sm211* animals²³. Most cell corpses in wild-type animals persisted for 10–40 min, with an average duration of 28 min (Fig. 1c). In contrast, most cell corpses in *sm211* embryos lasted for 30–110 min, with an average duration almost twice as long (55 min; Fig. 1c), indicating that cell corpse engulfment was compromised. Similar delayed and compromised cell corpse engulfment was observed in the *sm211* mutant in three specific cells (C1, C2 and C3; Fig. 1d), which are programmed to die at the mid-embryonic stage²⁴. We also counted the number of nuclei in the

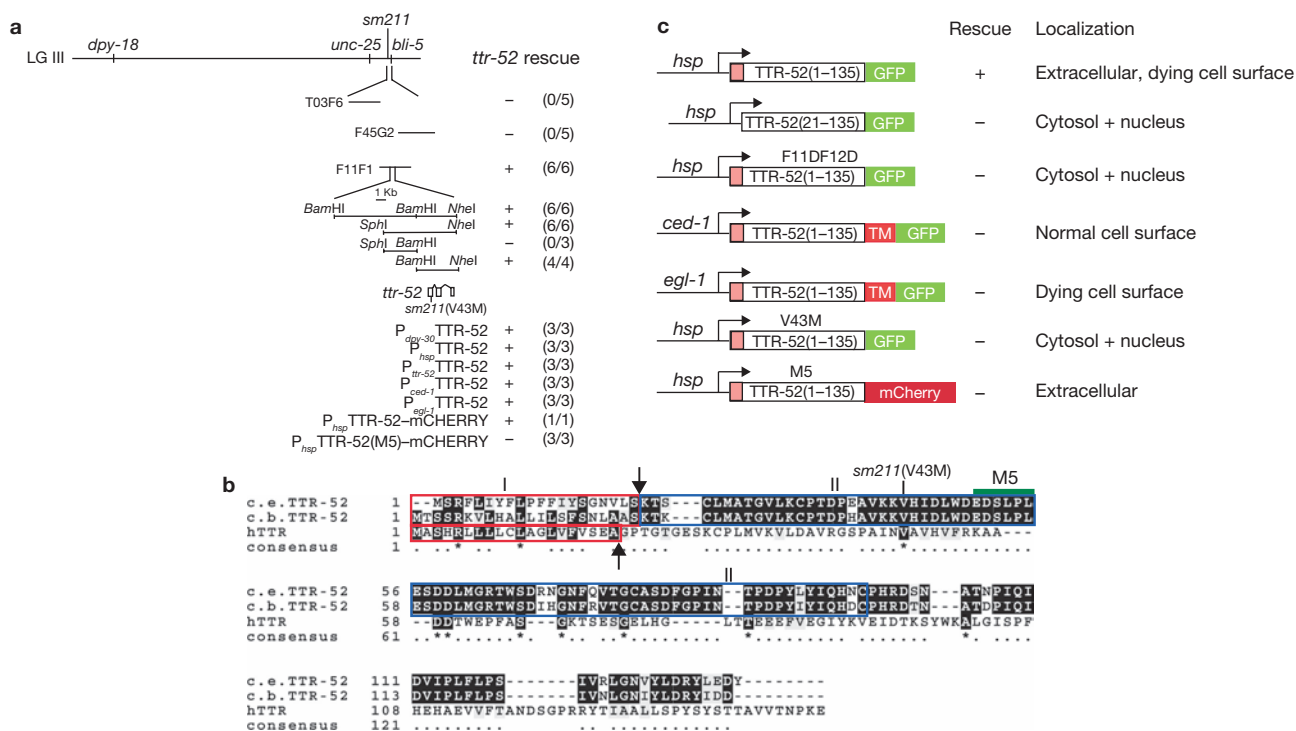


Figure 2 *ttr-52* encodes a secreted, transthyretin-like protein important for cell corpse engulfment. (a) Cloning of the gene affected by the *sm211* mutation. The mapped position of *sm211* on LG III and results of transformation rescue of the *sm211* mutant by various cosmids and constructs are shown. Cell corpses in 2-fold transgenic embryos were scored (15 embryos for each line). A plus sign indicates rescue, a minus sign no rescue. For each construct the number of independent transgenic lines that showed rescue and the number of transgenic lines tested are shown in parentheses. For *P_{hsp}* TTR-52-mCherry, the rescue was scored with an integrated array (*smIs119*) carrying this construct. (b) Sequence alignment of *C. elegans* (c.e.) and *C. briggsae* (c.b.) TTR-52 and human transthyretin

(hTTR). Identical residues are shaded in black, and similar residues in grey. Residues that are identical in all three proteins are marked with an asterisk. Box I indicates the predicted secretion signal; arrows point to the putative cleavage sites. Box II delineates the transthyretin-like domain. The mutation identified in the *ttr-52(sm211)* mutant and the residues mutated in TTR-52(M5) are indicated. (c) Secretion of TTR-52 is crucial for its function in cell corpse engulfment. The GFP or mCherry fusion constructs shown at the left were injected into wild-type and *ttr-52(sm211)* animals. The subcellular localization patterns of the fusion proteins and their ability to rescue the *ttr-52* mutant are shown on the right. A total of 15 animals each from three independent transgenic lines were scored for each construct.

anterior pharynx of *sm211* animals (see Methods) and found that they did not have any normally living cells missing or undergoing ectopic apoptosis in this region. Instead, a few cells that are normally programmed to die survived inappropriately in some *sm211* animals (Supplementary Information, Table S1), suggesting that *sm211* actually promotes cell survival. Indeed, *sm211* significantly enhances the cell death defect of the weak *ced-3* or *ced-4* loss-of-function (*lf*) mutants (Supplementary Information, Table S1), a phenomenon also observed with many engulfment-defective mutations such as *ced-1(lf)* mutations^{25,26}. Taken together, these results indicate that the cell corpse engulfment process is severely compromised in the *sm211* mutant.

ttr-52 acts in the *ced-1* pathway

We analysed double mutants containing *sm211* and strong *lf* mutations in genes involved in cell corpse engulfment to determine the engulfment pathway in which the gene affected by *sm211* acts. *sm211* specifically enhanced the engulfment defect conferred by mutations in the *ced-2*, *ced-5*, *ced-10* and *ced-12* genes, which act in one pathway, but not that caused by mutations in the *ced-1*, *ced-6* and *ced-7* genes, which act in a different engulfment pathway (Fig. 1e). These results indicate that the gene affected by *sm211* probably functions in the same corpse engulfment pathway as *ced-1*, *ced-6* and *ced-7*.

We mapped *sm211* very close to the *bli-5* gene on linkage group III (LG III, Fig. 2a; see Methods). Transformation rescue experiments revealed

that one cosmid in the mapped region, F11F1, fully rescued the engulfment defect of the *sm211* mutant. Subclones of F11F1 were made and a 3.7-kilobase (kb) *Bam*HI-*Nhe*I genomic fragment was capable of rescuing the *sm211* mutant (Fig. 2a). There is only one gene in this region, *ttr-52* (transthyretin-related family domain), which encodes a 135-residue protein that shares limited sequence similarity to transthyretin (Fig. 2b), a thyroid-hormone-binding protein found in the blood of vertebrates²⁷. TTR-52 is one of the 57 transthyretin-like proteins in *C. elegans*^{28,29}, each of which contains a transthyretin-like domain (Pfam ID: PF01060) (Supplementary Information, Fig. S1). The biological functions of this gene family are unknown, and most are predicted to encode secretory proteins (Supplementary Information, Table S2). We identified a G→A transition in the *ttr-52* gene from the *sm211* mutant, which results in the replacement of Val 43 by Met, a conserved residue among worm TTR proteins and human transthyretin (Fig. 2b; Supplementary Information, Fig. S1). Expression of a full-length *ttr-52* complementary DNA under the control of several different *C. elegans* gene promoters fully rescued the *sm211* mutant (Fig. 2a), confirming that *ttr-52* is the gene affected by *sm211*.

TTR-52 is a secretory protein that binds apoptotic cells

Protein sequence analysis revealed that TTR-52 contains a secretion signal at its amino terminus (Fig. 2b). To determine the cellular localization pattern of TTR-52, we expressed a TTR-52-GFP fusion under the control

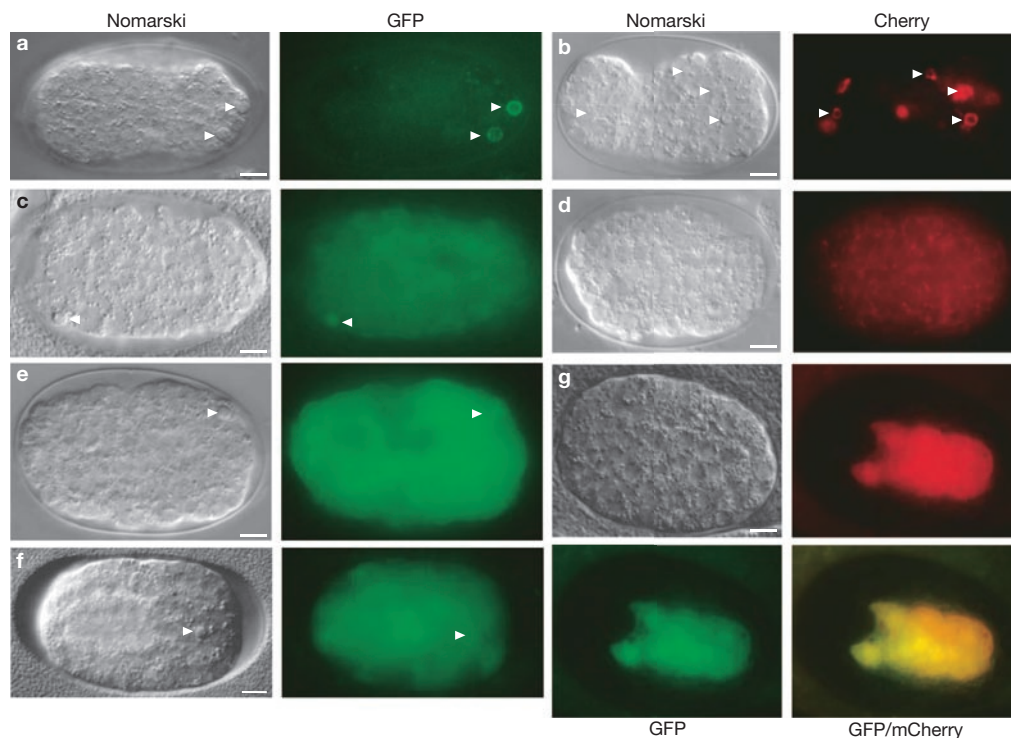


Figure 3 TTR-52 is expressed in and secreted from intestine cells and binds to the surface of apoptotic cells. (a–f) Localization patterns of various TTR-52 GFP or mCherry fusions. Nomarski and GFP or mCherry images of a wild-type *C. elegans* embryo transgenic for P_{hsp} TTR-52–GFP (a), P_{hsp} TTR-52–mCherry (b), P_{hsp} TTR-52(21–135)–GFP (c), P_{hsp} TTR-52(F11D F12D)–GFP (e) and P_{hsp} TTR-52(V43M)–GFP (f) and a *ced-3(n717)* embryo carrying P_{hsp} TTR-52–mCherry

(d) are shown. Apoptotic cells displaying raised disc-like morphology in Nomarski images are indicated with arrowheads. Exposure times were 2,000 ms (a), 3,000 ms (c, e, f) and 500 ms (b, d). (g) *ttr-52* is expressed in intestine cells. Nomarski, mCherry and GFP images and the merged image of a wild-type embryo transgenic for both P_{ttr-52} –mCherry and P_{ges-1} –GFP are shown. Scale bars, 5 μ m. Three independent transgenic lines were examined for each experiment.

of the *C. elegans* heat-shock promoters (P_{hsp} TTR-52–GFP), which fully rescued the engulfment defect of the *ttr-52(sm211)* mutant (Fig. 2c). On heat-shock treatment, TTR-52–GFP was detected almost exclusively on the surface of apoptotic cells, showing a bright ring-like staining (Figs 2c and 3a). In some embryos, weak GFP staining was also observed on the surface of cells adjacent to the dying cells (Supplementary Information, Fig. S2a). Because heat-shock promoters induce global gene expression in *C. elegans* embryos, this unique, restricted TTR-52 localization pattern indicates that TTR-52 may be a secretory protein that binds rather specifically to the surface of apoptotic cells. Expression of a TTR-52–mCherry (monomeric Cherry) fusion under the control of the heat-shock promoters or the *ttr-52* promoter resulted in the same staining pattern (Fig. 3b). The staining of TTR-52–mCherry or TTR-52–GFP on the surface of dying cells was abolished by a loss-of-function mutation in the *ced-3* gene (*n717*) (Fig. 3d; data not shown), which blocks almost all apoptosis in *C. elegans*³⁰, confirming that the cells labelled by TTR-52 were apoptotic cells.

To confirm that TTR-52 is a secretory protein, we generated two mutant TTR-52–GFP fusions, TTR-52(21–135)–GFP and TTR-52(F11D, F12D)–GFP, and expressed them under the control of heat-shock promoters (Fig. 2c; Supplementary Information, Fig. S3). The first of these lacks the predicted secretion signal (residues 1–20) and the latter contains mutations altering two hydrophobic residues in the signal peptide that are predicted to be critical for the secretion of the protein (SignalP 3.0 program; <http://www.cbs.dtu.dk/services/SignalP/>). In embryos expressing these two mutant TTR-52–GFP fusions, the

surface of apoptotic cells was not labelled by GFP. Instead, diffused GFP was observed in the cytosol and nucleus of both apoptotic and non-apoptotic cells, indicating that they are not secreted (Fig. 3c, e; Supplementary Information, Fig. S4a, b). We observed a similar GFP staining pattern with TTR-52–GFP carrying the V43M mutation found in the *sm211* mutant (Fig. 3f; Supplementary Information, Figs S3e and S4c). All three TTR-52–GFP fusions failed to rescue the engulfment defect of the *ttr-52(sm211)* mutant (Fig. 2c). TTR-52 therefore needs to be secreted to function.

We also tested whether TTR-52 could function properly when tethered to the cell surface. We generated a transmembrane TTR-52–GFP fusion (TTR-52–TM–GFP) by inserting the transmembrane domain of CED-1 between TTR-52 and GFP and expressed this fusion in either engulfing cells or dying cells under the control of the *ced-1* or *egl-1* promoter (Fig. 2c)^{10,31}. In embryos transgenic for P_{ced-1} TTR-52–TM–GFP or P_{egl-1} TTR-52–TM–GFP, the GFP fusion was found on the surface of normal and dying cells, respectively (Fig. 2c; Supplementary Information, Fig. S2c; data not shown). However, TTR-52–TM–GFP expressed in engulfing cells did not cluster around apoptotic cells in the same way as TTR-52–GFP (Supplementary Information, Fig. S2c), suggesting that membrane tethering affects or interferes with recognition of apoptotic cells by TTR-52. Indeed, neither of the constructs alone or in combination rescued the engulfment defect of the *ttr-52(sm211)* mutant (Fig. 2c; data not shown). In comparison, expression of TTR-52 under the control of the same promoters (P_{ced-1} TTR-52 or P_{egl-1} TTR-52) fully rescued the *ttr-52(sm211)* mutant (Fig. 2a), indicating that the membrane-tethered TTR-52 cannot substitute for a secreted TTR-52.

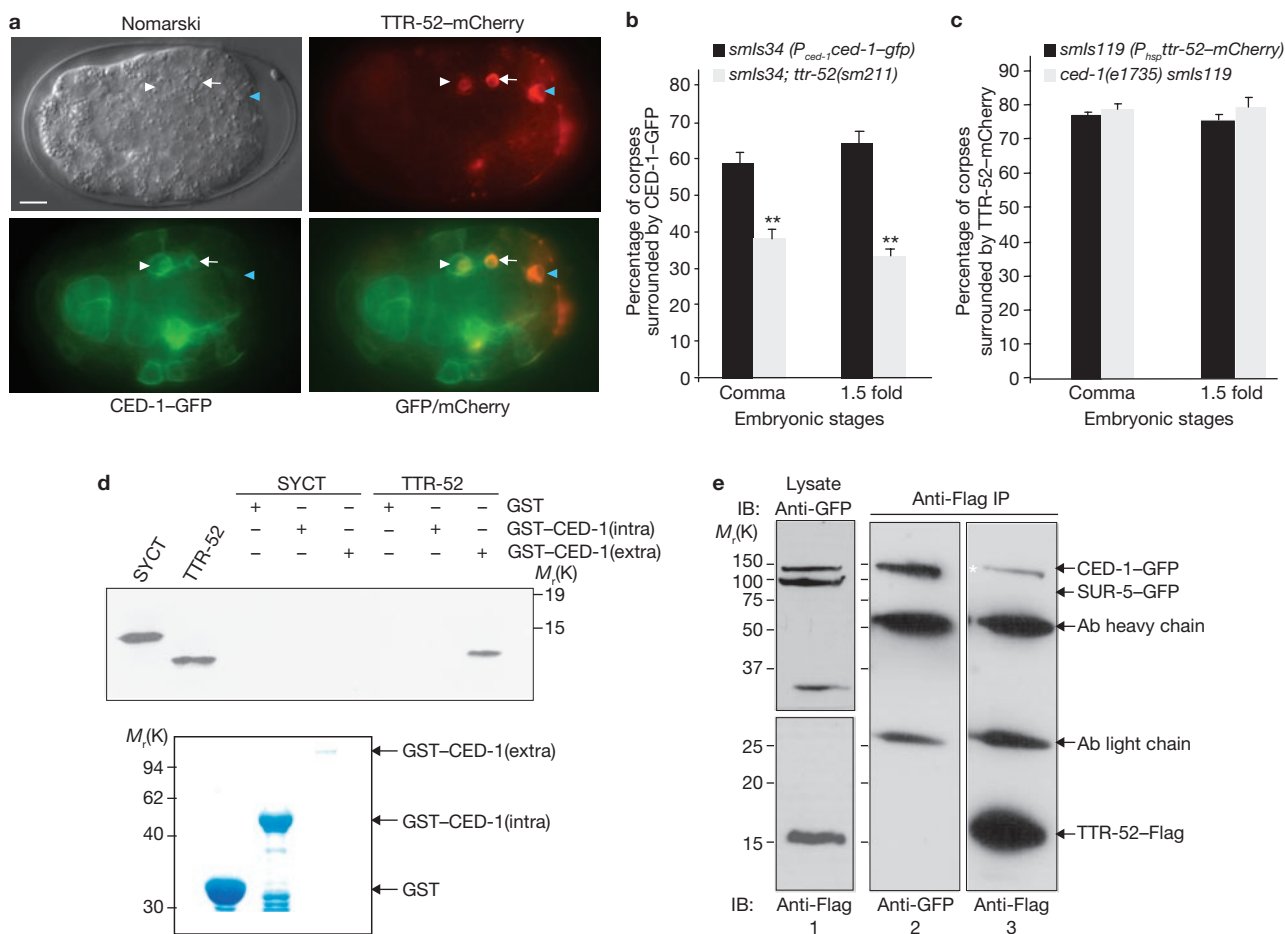


Figure 4 TTR-52 and CED-1 interact and co-localize to apoptotic cells. **(a)** Nomarski, mCherry and GFP images and the merged image of an early N2 embryo carrying both P_{ttr-52} TTR-52-mCherry and P_{ced-1} CED-1-GFP. TTR-52-mCherry and CED-1-GFP formed a completely overlapping ring surrounding dying cells (arrow), which was sometimes already internalized by a phagocyte (arrowhead). TTR-52-mCherry could label a dying cell alone (blue arrowhead). Scale bar, 5 μ m. **(b)** *ttr-52* partly mediates the binding of CED-1 to apoptotic cells. The percentage of cell corpses surrounded by CED-1-GFP was determined in the indicated strains by analysing serial optical sections of embryo (see Methods). Two asterisks, $P < 0.0001$. **(c)** The binding of TTR-52 to apoptotic cells was not affected by loss of *ced-1*. The percentage of cell corpses surrounded by TTR-52-mCherry was scored in the indicated strains as described in **b**. In **b** and **c** a total of 15 embryos each at the comma and 1.5-fold embryonic stages were scored. Error bars indicate s.e.m. **(d)** TTR-52 interacts with the extracellular domain (Extra) of CED-1. Purified GST, GST-CED-1(Extra) and GST-CED-1(Intra) (1 μ g of each) immobilized on glutathione-agarose beads were incubated with TTR-52(21-135)-His₆ or

a control protein SYCT-His₆. The bound proteins were resolved on a 15% SDS-polyacrylamide gel and revealed by immunoblotting with antibodies against a hexahistidine tag. Purified GST fusion proteins stained with Coomassie blue are shown underneath. Four independent experiments were performed. **(e)** CED-1 interacts with TTR-52 *in vivo*. A co-IP experiment was performed in *ced-5(n1812)* animals co-expressing CED-1-GFP, TTR-52-Flag and SUR-5-GFP (see Methods). An antibody against the Flag epitope pulled down CED-1-GFP, but not SUR-5-GFP, with TTR-52-Flag; these were revealed by immunoblotting (IB) first with an anti-GFP antibody (lane 2) and then reprobing with an anti-Flag antibody after the same blot had been stripped of antibodies (lane 3; see Methods). In lane 3 the residual CED-1-GFP band observed (indicated with an asterisk) is due to incomplete stripping of antibodies. Lane 1 shows the expression levels of three fusion proteins in the worm lysate used for IP. The blot was cut into two halves; one was used for anti-GFP immunoblotting (top) and the other was used for anti-Flag immunoblotting (bottom). Three independent experiments were performed. Uncropped images of blots are shown in Supplementary Information, Fig. S6.

To examine where *ttr-52* is expressed in *C. elegans*, we generated a *ttr-52* transcriptional fusion with mCherry (P_{ttr-52} mCherry) and found that the *ttr-52* promoter drove mCherry expression specifically in intestine cells, which completely overlapped with the GFP expression pattern of P_{ges-1} GFP, an intestine-specific reporter construct (Fig. 3g)³². Therefore, the intestine cells, which do not undergo programmed cell death in *C. elegans*^{33,34}, synthesize TTR-52, which probably is secreted, diffuses and binds to apoptotic cells, promoting their engulfment by neighbouring phagocytes. Consistent with this notion, when TTR-52-mCherry and GFP were co-expressed under the control of the endogenous *ttr-52* promoter (P_{ttr-52} TTR-52-mCherry and P_{ttr-52} GFP),

GFP expression was restricted to the gut, whereas TTR-52-mCherry was seen mostly outside the gut region, labelling apoptotic cells that were either close to or far from the gut (Supplementary Information, Fig. S2d).

TTR-52 mediates recognition of apoptotic cells by CED-1

ced-1 encodes a phagocyte receptor that clusters around apoptotic cells through an unknown mechanism¹⁰. The observations that TTR-52, a secreted protein, similarly clusters around apoptotic cells and acts in the same engulfment pathway as CED-1 suggest that TTR-52 may function to mediate the recognition of dying cells by CED-1. Indeed, in a

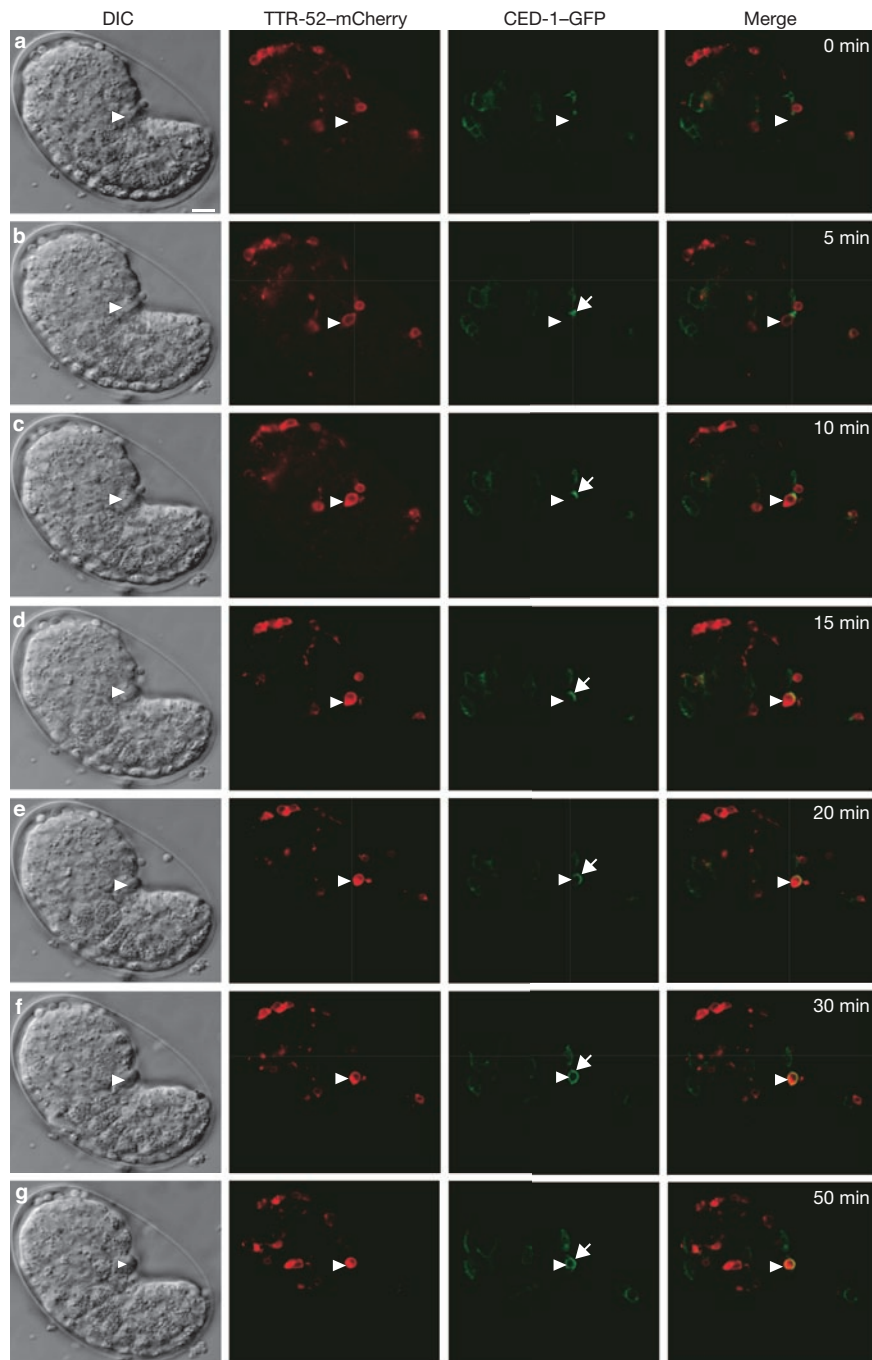


Figure 5 Clustering of TTR-52 and CED-1 around apoptotic cells monitored by time-lapse microscopy. (a–g) Confocal images of Nomarski (differential interference contrast (DIC)), TTR-52-mCherry and CED-1-GFP and the merged images of mCherry and GFP of a wild-type embryo carrying both P_{hsp} TTR-52-mCherry and P_{ced-1} CED-1-GFP at various time points. TTR-

52-mCherry formed a complete ring surrounding the dying cell early during apoptosis (arrowhead in b), whereas a CED-1-GFP ring (indicated by an arrow) was formed gradually (b–e) and completed 25 min later (f). Scale bar, 5 μ m. Similar sequential clustering of TTR-52 and CED-1 around apoptotic cells was observed in 37 cell corpses (eight embryos) by time-lapse recordings.

strain expressing both TTR-52-mCherry (P_{hsp} TTR-52-mCherry) and CED-1-GFP (P_{ced-1} CED-1-GFP), TTR-52-mCherry frequently co-localized with CED-1-GFP, because 69% of apoptotic cells clustered by CED-1-GFP were also surrounded by TTR-52-mCherry ($n = 183$). TTR-52-mCherry and CED-1-GFP formed either an overlapping mCherry/GFP ring around the apoptotic cell (indicated by an arrow in Fig. 4a) or an mCherry/GFP ring inside a larger CED-1-GFP ring,

indicative of an internalized apoptotic cell in a phagocyte (indicated by an arrowhead in Fig. 4a). TTR-52-mCherry rings were also seen alone (indicated by a blue arrowhead in Fig. 4a) or accompanied by a partial or incomplete CED-1-GFP ring (Fig. 5b–e), indicating that formation of the TTR-52-mCherry ring precedes the formation of a CED-1-GFP ring on apoptotic cells. By time-lapse microscopy analysis, we observed that a complete TTR-52-mCherry ring was formed rapidly around the

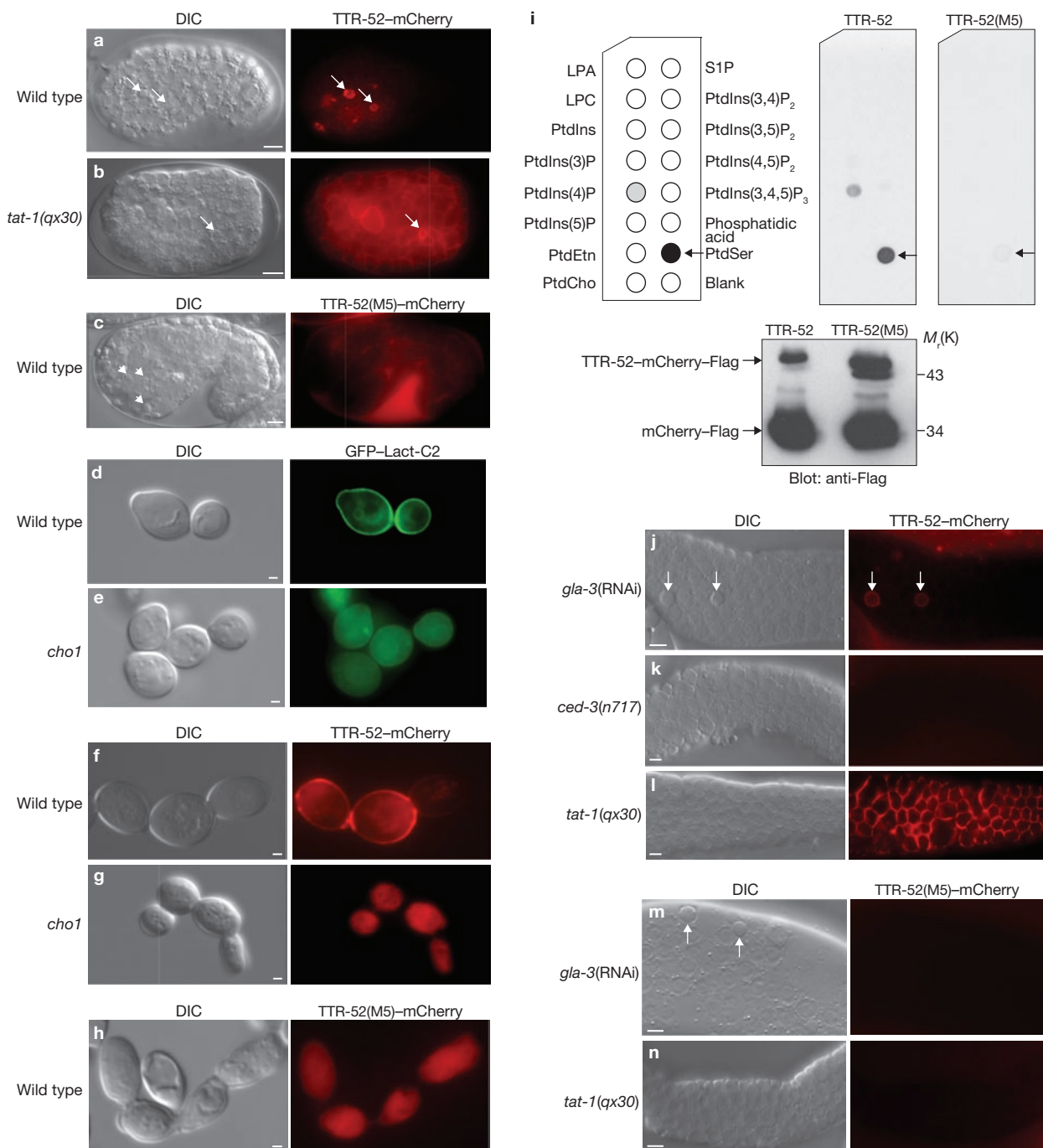


Figure 6 TTR-52 binds surface-exposed PtdSer. (a–c) Nomarski (left) and mCherry (right) images of a wild-type embryo carrying P_{hsp} TTR-52-mCherry (a) and P_{hsp} TTR-52(M5)-mCherry (c), and a *tat-1(qx30)* mutant embryo carrying P_{hsp} TTR-52-mCherry (b) are shown. TTR-52-mCherry formed bright rings specifically around dying cells in the wild-type embryo (indicated by arrows in a) but appeared on the surface of virtually all cells in the *tat-1(qx30)* embryo (b). TTR-52(M5)-mCherry failed to label apoptotic cells (arrowheads in c). More than 100 embryos were examined for each panel. Exposure times were 500 ms. Scale bars, 5 μ m. (d–h) TTR-52 binds PtdSer in yeast plasma membrane. Nomarski, GFP and mCherry images of wild-type yeast cells expressing GFP-Lact-C2 (d), TTR-52-mCherry (f) and TTR-52(M5)-mCherry (h) and images of PtdSer-deficient yeast cells (*cho1*) expressing GFP-Lact-C2 (e) and TTR-52-mCherry (g) are shown. Three independent experiments were performed for each construct. Scale bars, 1 μ m. (i) TTR-52 binds PtdSer *in vitro*. Affinity-purified TTR-52-mCherry-Flag, but not TTR-52(M5)-mCherry-Flag, bound PtdSer

spotted on a membrane strip (indicated by arrows; see Methods). TTR-52 also showed weak binding to phosphatidylinositol-4-phosphate (PtdIns(4)P). The amounts of purified TTR-52 proteins used in lipid binding were shown by immunoblotting (bottom panel). Two independent experiments were performed. LPA, lysophosphatidic acid; LPC, lysophosphatidylcholine; S1P, sphingosine-1-phosphate. (j–n) TTR-52 binds apoptotic cells *ex vivo*. Dissected gonads from the indicated strains were incubated with purified TTR-52-mCherry-Flag or TTR-52(M5)-mCherry-Flag (see Methods). Nomarski and mCherry images of dissected gonads are shown. TTR-52 specifically labelled apoptotic germ cells (indicated by arrows) in *gla-3(RNAi)* animals (j) but stained many germ cells in the *tat-1(qx30)* mutant (l). No TTR-52 labelling was observed in the *ced-3(n717)* mutant, which lacks germ-cell death (k). TTR-52(M5) failed to label any germ cell in *gla-3(RNAi)* animals (m) or *tat-1(qx30)* animals (n). Scale bars, 5 μ m. At least 30 gonads were examined for each experiment. Uncropped images of blots are shown in Supplementary Information, Fig. S6.

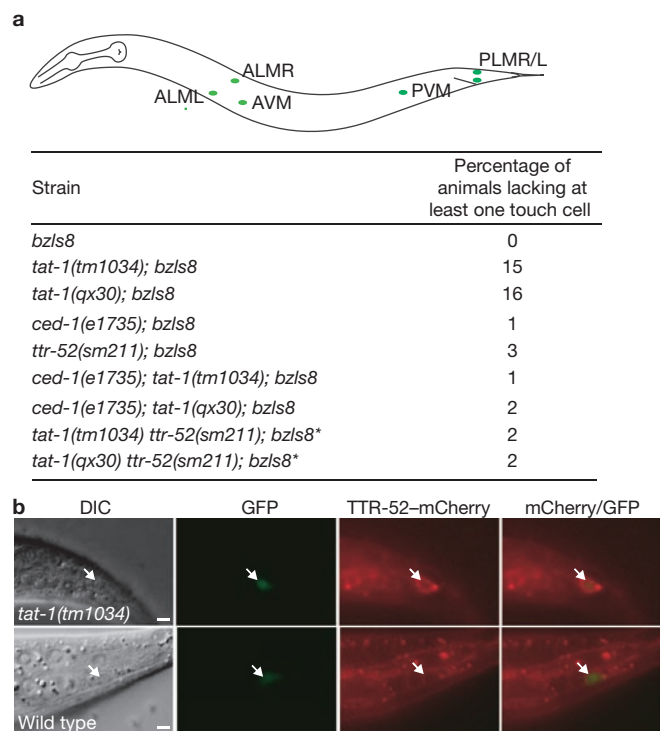


Figure 7 TTR-52 mediates the random removal of neurons with surface-exposed PtdSer. (a) An integrated GFP reporter line, *bzIs8*, labels six touch-receptor neurons (indicated with green dots). The presence of neurons was scored by using a Nomarski microscope with epifluorescence; the percentages of animals lacking one or more neurons are shown. A total of 90 animals were scored for each strain. Strains marked with an asterisk also contain the *dpy-18(e364)* mutation. (b) TTR-52 labels the surface of the PLM (posterior lateral microtubule) touch cell in the *tat-1* mutant. Nomarski, GFP and mCherry images and the merged images of GFP and mCherry of a wild-type or *tat-1(tm1034)* larva carrying both P_{hsp} TTR-52-mCherry (*smIs119*) and P_{mec-1} GFP (*bzIs8*) transgenes are shown. TTR-52-mCherry labelled only the surface of the PLM touch cell in the *tat-1(tm1034)* mutant. Scale bars, 5 μ m. A total of 20 animals were examined for each strain.

dying cell early during apoptosis (indicated by an arrowhead in Fig. 5b), whereas only trace amounts of CED-1-GFP were seen nearby (indicated by an arrow in Fig. 5b). CED-1-GFP continued to circularize (Fig. 5c–e) and formed a complete circle overlapping the TTR-52-mCherry ring within 30 min (Fig. 5f). In 37 apoptotic cells from eight embryos that we monitored, the TTR-52-mCherry ring was always formed before the CED-1-GFP ring, indicating that TTR-52 might induce the formation of the CED-1-GFP ring around apoptotic cells.

We therefore examined whether loss of *ttr-52* affects the clustering of CED-1-GFP around apoptotic cells by analysing *C. elegans* embryos expressing CED-1-GFP (*smIs34*; P_{ced-1} CED-1-GFP). About 64% of cell corpses were labelled by CED-1-GFP in wild-type 1.5-fold-stage embryos. By contrast, in *smIs34; ttr-52(sm211)* 1.5-fold-stage embryos, only half (34%) of the cell corpses were labelled (Fig. 4b), indicating that TTR-52 is important for mediating the clustering of CED-1 around apoptotic cells. Because clustering of apoptotic cells by TTR-52-mCherry was not affected by a loss of *ced-1* (Fig. 4c), these results indicate that TTR-52 is independent of and precedes CED-1 in binding to apoptotic cells.

We examined whether TTR-52 interacts directly with CED-1 *in vitro*, using a glutathione S-transferase (GST) fusion protein pulldown assay. Recombinant TTR-52 interacted with purified GST-CED-1(Extra),

which contains the extracellular domain of CED-1, but not with either GST or GST-CED-1(Intra), which contains the intracellular domain of CED-1 (Fig. 4d). None of these GST fusion proteins bound SYCT (specific Yop chaperone), a control protein, suggesting that TTR-52 interacts specifically with the extracellular domain of CED-1. We also examined the interaction of TTR-52 with CED-1 by co-immunoprecipitation (co-IP) assays with a *C. elegans* strain that co-expressed CED-1-GFP from *smIs34* and TTR-52-Flag and SUR-5-GFP from a second integrated transgene *smIs118* (carrying both P_{hsp} TTR-52-Flag and P_{sur-5} SUR-5-GFP) (Fig. 4e, lane 1). Using an antibody against the Flag epitope, CED-1-GFP but not SUR-5-GFP was specifically co-precipitated with TTR-52-Flag (Fig. 4e, lanes 2 and 3). Taken together, these results indicate that TTR-52 interacts specifically with the CED-1 receptor to mediate the recognition and binding of apoptotic cells by CED-1.

TTR-52 recognizes surface-exposed PtdSer

To identify the apoptotic cell signal recognized by TTR-52, we performed a genetic screen to search for mutations that altered the staining of TTR-52-mCherry to apoptotic cells. One mutation, *qx30*, resulted in TTR-52-mCherry staining of virtually all cells in *qx30* mutant embryos, including non-apoptotic cells that are normally not labelled by TTR-52 (Fig. 6a, b). *qx30* turns out to be an allele of *tat-1* (see Methods), which encodes an aminophospholipid translocase that prevents the appearance of PtdSer in the outer leaflet of the plasma membrane²². Because in *tat-1(lf)* animals PtdSer is ectopically exposed on the surface of many living cells²², this unexpected finding suggests that TTR-52 may bind surface-exposed PtdSer.

We employed a yeast-based PtdSer binding assay³⁵ to test the binding of TTR-52 to PtdSer. In this assay the C2 domain of lactadherin (Lact-C2), which binds specifically to PtdSer³⁶, associates predominantly with plasma membrane that contains PtdSer in its inner leaflet in wild-type yeast cells (Fig. 6d)³⁵. In *cho1* mutant cells, which are deficient in PtdSer synthesis, GFP-Lact-C2 becomes cytosolic (Fig. 6e), because of a loss of PtdSer in yeast plasma membrane³⁵. Like GFP-Lact-C2, TTR-52-mCherry labelled plasma membrane in wild-type yeast cells but failed to do so in the *cho1* cells (Fig. 6f, g), indicating that TTR-52 binds PtdSer in plasma membrane.

To identify the region of TTR-52 that is important for PtdSer binding, we generated several TTR-52 mutants with mutations or small deletions (data not shown). One mutant, TTR-52(M5), in which residues 50–55 were replaced by alanines, failed to associate with yeast plasma membrane (Figs 2b and 6h), presumably because of a loss of PtdSer binding. *In vivo*, TTR-52(M5)-mCherry failed to rescue the engulfment defect of the *ttr-52(sm211)* mutant and did not cluster around apoptotic cells in wild-type embryos (Figs 2c and 6c; Supplementary Fig. 3i), although it was secreted normally and accumulated in the embryo cavity.

We also examined whether TTR-52 binds PtdSer and apoptotic cells directly. Recombinant TTR-52-mCherry-Flag was purified from human 293T cells and tested for binding to a membrane strip spotted with 16 different phospholipids (see Methods). TTR-52 showed strong and specific binding to PtdSer but not to other phospholipids such as phosphatidylcholine, phosphatidylethanolamine, phosphatidic acid and various phosphoinositides, with the exception of a weak binding to phosphatidylinositol-4-phosphate (Fig. 6i). In contrast, the binding of TTR-52(M5)-mCherry-Flag to PtdSer was barely detectable. Thus, TTR-52 binds specifically to PtdSer *in vitro*.

When we incubated purified TTR-52-mCherry-Flag with dissected gonads from animals treated with *gla-3* RNA-mediated interference

(RNAi), which causes increased germ-cell deaths³⁷, TTR-52–mCherry specifically labelled apoptotic germ cells on the surface of the dissected gonad (Fig. 6j)¹⁹. This TTR-52 labelling was abolished by the *ced-3(n717)* mutation (Fig. 6k), indicating that TTR-52 binds apoptotic germ cells. TTR-52–mCherry also stained many germ cells in the *tat-1(qx30)* mutant (Fig. 6l), in which PtdSer is ectopically exposed on the surface of normal germ cells²². In contrast, purified TTR-52(M5)–mCherry failed to label apoptotic germ cells in *gla-3(RNAi)* animals and normal germ cells in the *tat-1(qx30)* mutant (Fig. 6m, n). Taken together, these results indicate that TTR-52 binds surface-exposed PtdSer and thus mediates the recognition of apoptotic cells by the phagocyte receptor CED-1.

TTR-52 mediates engulfment of cells with surface-exposed PtdSer

One physiological consequence of ectopic PtdSer exposure on the surface of normal cells in *tat-1(lf)* animals is the random removal of these cells through a CED-1-dependent phagocytic mechanism²². For example, in *bzIs8* animals, six touch-receptor neurons were labelled by GFP expressed from the P_{mcc-4} GFP construct carried by the integrated *bzIs8* transgene, and none of the *bzIs8* animals lost touch cells (Fig. 7a). By contrast, 15–16% of *tat-1(qx30); bzIs8* or *tat-1(tm1034); bzIs8* animals lost at least one touch cell. This missing-cell phenotype was strongly suppressed by the *ced-1(e1735)* mutation (Fig. 7a), suggesting that CED-1 recognizes and mediates the removal of cells with surface-exposed PtdSer. The missing-cell phenotype of the *tat-1(lf)* mutants was also strongly suppressed by *ttr-52(sm211)* (Fig. 7a), despite its being a weaker engulfment-blocking mutation than *ced-1(e1735)*. This result suggests that TTR-52 solely mediates the recognition of surface-exposed PtdSer by CED-1, which could be the only engulfment signal expressed by touch cells in *tat-1(lf)* animals. Consistent with this finding, TTR-52–mCherry labelled the surface of touch cells in *tat-1(tm1034); bzIs8* animals, but not touch cells in *bzIs8* animals (Fig. 7b).

DISCUSSION

It is unknown how the CED-1 family of phagocyte receptors recognizes apoptotic cells; this is a subject of intense study. Here we have identified a new gene, *ttr-52*, that encodes a secretory protein and acts specifically in the CED-1 signalling pathway to mediate the engulfment of apoptotic cells in *C. elegans*. The secreted TTR-52 protein clusters around apoptotic cells and precedes CED-1 in binding to apoptotic cells *in vivo*. Moreover, TTR-52 is important for the efficient binding of CED-1 to apoptotic cells and interacts specifically with the extracellular domain of CED-1. These findings together provide strong evidence that TTR-52 is a new extracellular bridging molecule that mediates the binding and recognition of apoptotic cells by the phagocyte receptor CED-1.

How does CED-1 or TTR-52 recognize apoptotic cells? We found that TTR-52 binds plasma membrane PtdSer in a yeast-based PtdSer binding assay (Fig. 6f, g) and binds PtdSer specifically *in vitro* (Fig. 6i), indicating that it is a PtdSer-binding protein. Moreover, recombinant TTR-52 specifically labelled apoptotic germ cells and the surface of many germ cells in the *tat-1(lf)* mutant *ex vivo* (Fig. 6j–l), providing direct evidence that TTR-52 recognizes and binds surface-exposed PtdSer. A TTR-52 mutant, TTR-52(M5), that fails to bind PtdSer *in vitro* (Fig. 6i), loses its ability to bind apoptotic cells in *C. elegans* and its activity in rescuing the engulfment defect of the *ttr-52(sm211)* mutant (Figs 2 and 6), indicating that the ability to bind PtdSer is critical for the function of TTR-52 in phagocytosis. Like CED-1, TTR-52 is required for the removal of normal

cells with inappropriately exposed PtdSer in the *tat-1(lf)* mutants (Fig. 7), which presumably do not express other 'eat-me' signals seen on the surface of apoptotic cells²². TTR-52 therefore most probably recognizes and binds surface-exposed PtdSer to mediate cell corpse engulfment. Given that surface-exposed PtdSer is the only conserved engulfment signal so far identified in multiple organisms¹⁸, it may serve as a conserved recognition signal for the CED-1 receptor family.

In mammals, extracellular bridging molecules such as thrombospondin (TSP), β_2 glycoprotein I and the collectin family proteins^{38–44}, some of which recognize and bind surface-exposed PtdSer, are important in crosslinking apoptotic cells to macrophages, which are often not in close contact with their targets. For invertebrate animals such as *Drosophila* and *C. elegans*, it is unclear whether bridging molecules are needed to mediate the removal of apoptotic cells, especially in *C. elegans*, in which phagocytes are neighbouring cells already in close contact with apoptotic cells. Our finding that TTR-52, an extracellular bridging protein, is important in mediating the recognition and binding of apoptotic cells by the CED-1 phagocyte receptor suggests that this is a conserved and important mechanism for the clearance of apoptotic cells, although the identities of bridging molecules could differ significantly across the species.

TTR-52 is a member of the transthyretin-like protein family, a sub-family of the larger transthyretin-related protein family (TRPs) that has sequence and structural similarity with transthyretin in the signature transthyretin-like domain and that has been found in a broad range of species, including bacteria, plants, invertebrates and vertebrates^{45,46}. The functions of TRPs are largely unknown, although some have been implicated in purine catabolism in mice and regulation of the brassinosteroid receptor in plants^{45–48}. There are 57 transthyretin-like proteins in *C. elegans*; their biological functions have not been characterized. TTR-52 is the first of this protein family with a clearly defined cellular function. Because many of the nematode transthyretin-like proteins are predicted to be secretory proteins (Supplementary Information, Table S2), it seems likely that one potential important function of this protein family is to act extracellularly to mediate cell–cell interaction, although individual RNAi knockdown of 57 worm transthyretin-like genes, including *ttr-52*, fails to reveal an obvious defect (data not shown). Because *ttr-52(sm211)* only partly blocks the clustering of CED-1 around apoptotic cells and causes a weaker engulfment defect than *ced-1(lf)* mutations, one or more additional bridging molecules and/or 'eat-me' signals could act in parallel to TTR-52 to mediate the recognition of apoptotic cells by CED-1. Furthermore, given the presence of multiple PtdSer-recognizing receptors in mammals⁴⁹, additional PtdSer-recognizing receptors, including PSR-1 (ref. 23), could act in parallel to TTR-52/CED-1 in *C. elegans* to mediate the removal of apoptotic cells with surface-exposed PtdSer. □

METHODS

Methods and any associated references are available in the online version of the paper at <http://www.nature.com/naturecellbiology/>

Note: Supplementary Information is available on the Nature Cell Biology website.

ACKNOWLEDGEMENTS

We thank J. McGhee for the P_{gcs-1} GFP construct and T. Blumenthal for comments and discussion on the manuscript. This work was supported by a Burroughs Wellcome Fund Award (D.X.), NIH R01 grants GM59083 and GM79097 (D.X.), and the National High Technology Project 863 of China (X.C.W.).

AUTHOR CONTRIBUTIONS

X.C.W. and W.D.L. performed most of the genetic and cell biological experiments. D.F.Z. performed both PtdSer binding experiments and *in vitro* protein interaction assays. Y.S. performed immunoprecipitation experiments in *C. elegans*. B.L., B.H.C., P.F.G. and X.G. performed some of the genetic and cell biological experiments. H.W.Y. performed the initial *in vitro* PtdSer binding experiments and E. P. conducted a bioinformatic analysis of TTR family proteins. Z.H.S., E.K.N. and S.M. contributed to the generation of strains. X.C.W. and D.X. designed the experiments and wrote the paper.

COMPETING FINANCIAL INTERESTS

The authors declare no competing financial interests.

Published online at <http://www.nature.com/naturecellbiology>

Reprints and permissions information is available online at <http://npg.nature.com/reprintsandpermissions/>

- Savill, J., Dransfield, I., Gregory, C. & Haslett, C. A blast from the past: clearance of apoptotic cells regulates immune responses. *Nat. Rev. Immunol.* **2**, 965–975 (2002).
- Henson, P. M., Bratton, D. L. & Fadok, V. A. Apoptotic cell removal. *Curr. Biol.* **11**, R795–R805 (2001).
- Savill, J. & Fadok, V. Corpse clearance defines the meaning of cell death. *Nature* **407**, 784–788 (2000).
- Reddien, P. W. & Horvitz, H. R. The engulfment process of programmed cell death in *Caenorhabditis elegans*. *Annu. Rev. Cell Dev. Biol.* **20**, 193–221 (2004).
- Reddien, P. W. & Horvitz, H. R. CED-2/CrkII and CED-10/Rac control phagocytosis and cell migration in *Caenorhabditis elegans*. *Nat. Cell Biol.* **2**, 131–136 (2000).
- Wu, Y. C. & Horvitz, H. R. *C. elegans* phagocytosis and cell-migration protein CED-5 is similar to human DOCK180. *Nature* **392**, 501–504 (1998).
- Gumienny, T. L. *et al.* CED-12/ELMO, a novel member of the CrkII/Dock180/Rac pathway, is required for phagocytosis and cell migration. *Cell* **107**, 27–41 (2001).
- Zhou, Z., Caron, E., Hartwig, E., Hall, A. & Horvitz, H. R. The *C. elegans* PH domain protein CED-12 regulates cytoskeletal reorganization via a Rho/Rac GTPase signaling pathway. *Dev. Cell* **1**, 477–489 (2001).
- Wu, Y. C., Tsai, M. C., Cheng, L. C., Chou, C. J. & Weng, N. Y. *C. elegans* CED-12 acts in the conserved crkII/DOCK180/Rac pathway to control cell migration and cell corpse engulfment. *Dev. Cell* **1**, 491–502 (2001).
- Zhou, Z., Hartwig, E. & Horvitz, H. R. CED-1 is a transmembrane receptor that mediates cell corpse engulfment in *C. elegans*. *Cell* **104**, 43–56 (2001).
- Su, H. P. *et al.* Interaction of CED-6/GULP, an adapter protein involved in engulfment of apoptotic cells with CED-1 and CD91/low density lipoprotein receptor-related protein (LRP). *J. Biol. Chem.* **277**, 11772–11779 (2002).
- Hamon, Y. *et al.* Cooperation between engulfment receptors: the case of ABCA1 and MEGF10. *PLoS ONE* **1**, e120 (2006).
- Manaka, J. *et al.* Draper-mediated and phosphatidylserine-independent phagocytosis of apoptotic cells by *Drosophila* hemocytes/macrophages. *J. Biol. Chem.* **279**, 48466–48476 (2004).
- Kurant, E., Axelrod, S., Leaman, D. & Gaul, U. Six-microns-under acts upstream of Draper in the glial phagocytosis of apoptotic neurons. *Cell* **133**, 498–509 (2008).
- MacDonald, J. M. *et al.* The *Drosophila* cell corpse engulfment receptor Draper mediates glial clearance of severed axons. *Neuron* **50**, 869–881 (2006).
- Gardai, S. J. *et al.* Cell-surface calreticulin initiates clearance of viable or apoptotic cells through trans-activation of LRP on the phagocyte. *Cell* **123**, 321–334 (2005).
- Fadok, V. A. *et al.* Exposure of phosphatidylserine on the surface of apoptotic lymphocytes triggers specific recognition and removal by macrophages. *J. Immunol.* **148**, 2207–2216 (1992).
- Gardai, S. J., Bratton, D. L., Ogden, C. A. & Henson, P. M. Recognition ligands on apoptotic cells: a perspective. *J. Leukoc. Biol.* **79**, 896–903 (2006).
- Wang, X. *et al.* *C. elegans* mitochondrial factor WAH-1 promotes phosphatidylserine externalization in apoptotic cells through phospholipid scramblase SCRM-1. *Nature Cell Biol.* **9**, 541–549 (2007).
- Zullig, S. *et al.* Aminophospholipid translocase TAT-1 promotes phosphatidylserine exposure during *C. elegans* apoptosis. *Curr. Biol.* **17**, 994–999 (2007).
- Venegas, V. & Zhou, Z. Two alternative mechanisms that regulate the presentation of apoptotic cell engulfment signal in *Caenorhabditis elegans*. *Mol. Biol. Cell* **18**, 3180–3192 (2007).
- Darland-Ransom, M. *et al.* Role of *C. elegans* TAT-1 protein in maintaining plasma membrane phosphatidylserine asymmetry. *Science* **320**, 528–531 (2008).
- Wang, X. *et al.* Cell corpse engulfment mediated by *C. elegans* phosphatidylserine receptor through CED-5 and CED-12. *Science* **302**, 1563–1566 (2003).
- Yu, X., Odera, S., Chuang, C. H., Lu, N. & Zhou, Z. *C. elegans* Dynamin mediates the signaling of phagocytic receptor CED-1 for the engulfment and degradation of apoptotic cells. *Dev. Cell* **10**, 743–757 (2006).
- Hoepfner, D. J., Hengartner, M. O. & Schnabel, R. Engulfment genes cooperate with *ced-3* to promote cell death in *Caenorhabditis elegans*. *Nature* **412**, 202–206 (2001).
- Reddien, P. W., Cameron, S. & Horvitz, H. R. Phagocytosis promotes programmed cell death in *C. elegans*. *Nature* **412**, 198–202 (2001).
- Schreiber, G. The evolutionary and integrative roles of transthyretin in thyroid hormone homeostasis. *J. Endocrinol.* **175**, 61–73 (2002).
- Sonnhammer, E. L. & Durbin, R. Analysis of protein domain families in *Caenorhabditis elegans*. *Genomics* **46**, 200–216 (1997).
- Saverwyns, H. *et al.* Analysis of the transthyretin-like (TTL) gene family in *Ostertagia ostertagi* — comparison with other stronglyid nematodes and *Caenorhabditis elegans*. *Int. J. Parasitol.* **38**, 1545–1556 (2008).
- Ellis, H. M. & Horvitz, H. R. Genetic control of programmed cell death in the nematode *C. elegans*. *Cell* **44**, 817–829 (1986).
- Conradt, B. & Horvitz, H. R. The TRA-1A sex determination protein of *C. elegans* regulates sexually dimorphic cell deaths by repressing the *egl-1* cell death activator gene. *Cell* **98**, 317–327 (1999).
- Kennedy, B. P. *et al.* The gut esterase gene (*ges-1*) from the nematodes *Caenorhabditis elegans* and *Caenorhabditis briggsae*. *J. Mol. Biol.* **229**, 890–908 (1993).
- Robertson, A. G. & Thomson, J. N. Morphology of programmed cell death in the ventral nerve chord of *C. elegans* larvae. *J. Embryol. Exp. Morphol.* **67**, 89 (1982).
- Sulston, J. E., Schierenberg, E., White, J. G. & Thomson, J. N. The embryonic cell lineage of the nematode *Caenorhabditis elegans*. *Dev. Biol.* **100**, 64–119 (1983).
- Yeung, T. *et al.* Membrane phosphatidylserine regulates surface charge and protein localization. *Science* **319**, 210–213 (2008).
- Shi, J., Heegaard, C. W., Rasmussen, J. T. & Gilbert, G. E. Lactadherin binds selectively to membranes containing phosphatidyl-L-serine and increased curvature. *Biochim. Biophys. Acta* **1667**, 82–90 (2004).
- Kritikou, E. A. *et al.* *C. elegans* GLA-3 is a novel component of the MAP kinase MPK-1 signaling pathway required for germ cell survival. *Genes Dev.* **20**, 2279–2292 (2006).
- Savill, J., Hogg, N., Ren, Y. & Haslett, C. Thrombospondin cooperates with CD36 and the vitronectin receptor in macrophage recognition of neutrophils undergoing apoptosis. *J. Clin. Invest.* **90**, 1513–1522 (1992).
- Anderson, H. A. *et al.* Serum-derived protein S binds to phosphatidylserine and stimulates the phagocytosis of apoptotic cells. *Nat. Immunol.* **4**, 87–91 (2003).
- Balasubramanian, K., Chandra, J. & Schroit, A. J. Immune clearance of phosphatidylserine-expressing cells by phagocytes. The role of β_2 -glycoprotein I in macrophage recognition. *J. Biol. Chem.* **272**, 31113–31117 (1997).
- Ishimoto, Y., Ohashi, K., Mizuno, K. & Nakano, T. Promotion of the uptake of PS liposomes and apoptotic cells by a product of growth arrest-specific gene, *gas6*. *J. Biochem. (Tokyo)* **127**, 411–417 (2000).
- Vandivier, R. W. *et al.* Role of surfactant proteins A, D, and C1q in the clearance of apoptotic cells *in vivo* and *in vitro*: calreticulin and CD91 as a common collectin receptor complex. *J. Immunol.* **169**, 3978–3986 (2002).
- Savill, J., Fadok, V., Henson, P. & Haslett, C. Phagocyte recognition of cells undergoing apoptosis. *Immunol. Today* **14**, 131–136 (1993).
- Gardai, S. J. *et al.* By binding SIRP α or calreticulin/CD91, lung collectins act as dual function surveillance molecules to suppress or enhance inflammation. *Cell* **115**, 13–23 (2003).
- Eneqvist, T., Lundberg, E., Nilsson, L., Abagyan, R. & Sauer-Eriksson, A. E. The transthyretin-related protein family. *Eur. J. Biochem.* **270**, 518–532 (2003).
- Lundberg, E., Backstrom, S., Sauer, U. H. & Sauer-Eriksson, A. E. The transthyretin-related protein: structural investigation of a novel protein family. *J. Struct. Biol.* **155**, 445–457 (2006).
- Lee, Y. *et al.* Mouse transthyretin-related protein is a hydrolase which degrades 5-hydroxyisourate, the end product of the uricase reaction. *Mol. Cells* **22**, 141–145 (2006).
- Nam, K. H. & Li, J. The *Arabidopsis* transthyretin-like protein is a potential substrate of BRASSINOSTEROID-INSENSITIVE 1. *Plant Cell* **16**, 2406–2417 (2004).
- Fadeel, B. & Xue, D. The ins and outs of phospholipid asymmetry in the plasma membrane: roles in health and disease. *Crit. Rev. Biochem. Mol. Biol.* **44**, 264–277 (2009).

METHODS

Strains and culture conditions. *C. elegans* strains were maintained with the use of standard methods⁵⁰. The N2 Bristol strain was used as the wild-type strain. All of the alleles used in this study have been described previously^{22,51,52}, except the *ced-12(n3261)* mutation⁸.

Isolation of the *ttr-52(sm211)* mutation. Standard ethylmethane sulphonate mutagenesis was performed on *sem-4(n1378); psr-1(tm469)* L4-stage hermaphrodites as described previously^{50,52}. Candidate F₁ adults that bag F₂ mutant progeny with many corpses at the 4-fold embryonic stage were rescued, and homozygous F₂ animals were recovered similarly by selecting for animals whose 4-fold-stage embryos contained persistent cell corpses. One of the mutants isolated was *sm211*, which was backcrossed with N₂ animals four times before further analysis.

Isolation of the *tat-1(qx30)* mutation. *qx30* is a recessive mutation isolated from a genetic screen looking for mutants in which TTR-52-mCherry failed to label apoptotic cells. It was mapped to LG III between genetic map positions 17.26 and 17.85, first by three-factor mapping with two genetic markers, *dpy-18* (8.65) and *bli-5* (21.21), and then by single nucleotide polymorphism mapping. Because the *tat-1* gene is at map position 17.59 of LG III, a transformation rescue experiment was performed and a DNA fragment containing the *tat-1* gene fully rescued the *qx30* defects. We identified a G→A transition in the *tat-1* gene from the *qx30* mutant that resulted in a premature stop codon after Leu 1028.

Quantification of cell corpses and extra cells. The numbers of cell corpses in the head region of living embryos or early L1 larvae and the number of extra cells in the anterior pharynx of L4 larvae were scored with the use of Nomarski optics as described previously⁵³.

Mapping of *sm211*. *sm211* was mapped to the right arm of LG III with *unc-36/dpy-18* and *dpy-18/unc-25* as three-factor mapping markers, respectively. In the third round of three-factor mapping, 38 out of 38 Dpy non-Bli recombinants from the *dpy-18(e364) bli-5(e518)/sm211* heterozygous mothers contained *sm211*, whereas 0 out of 55 Bli non-Dpy recombinants carried *sm211*. These results placed *sm211* to the right of or very close to the left of *bli-5*. Cosmids covering *bli-5* and the region to the right of *bli-5* were injected into *sm211* animals. One cosmid, F11F1, fully rescued the engulfment defect of the *sm211* mutant. Subclones of F11F1 were made; *ttr-52*, a gene defined by open reading frame F11F1.7, was found to possess the rescuing activity.

Fluorescence time-lapse microscopy. *C. elegans* embryos (300 min old) were mounted on slides with agar pad in egg salt buffer (118 mM NaCl, 48 mM KCl) and cover slips were sealed with beeswax and Vaseline (1:1). Images in a 26-μm z series (1.3 μm per section) were captured every 5 min for 150 min with a Zeiss LSM 5 Pascal inverted confocal microscope (Carl Zeiss MicroImaging, Inc.) and were processed and viewed with LSMImageBrowser software.

Quantification of CED-1-GFP clustered around apoptotic cells. To score the percentage of cell corpses labelled by CED-1-GFP, Nomarski and fluorescent images of embryos in a 20-μm z series (1 μm per section) were captured with a Zeiss Axioimager M1 equipped with epifluorescence and an AxioCam monochrome digital camera. Serial optical sections of embryos were analysed, first to identify cell corpses by their raised-disc-like morphology in comma-stage and 1.5-fold-stage embryos and then to determine the clustering of CED-1-GFP.

GST fusion protein pulldown assay. Purified GST, GST-CED-1(Extra) or GST-CED-1(Intra) (1 μg of each) immobilized on glutathione-agarose beads were incubated with 2.5 μg of TTR-52(21–135)-His₆ or SYCT-His₆ in a 100 μl reaction containing 25 mM Tris-HCl (pH 7.5), 150 mM NaCl, 0.1% Nonidet P40, 10% glycerol, 1 mM phenylmethylsulphonyl fluoride and 5 mM dithiothreitol at 4 °C. The beads were washed five times with the same buffer, and the bound proteins were resolved with a 15% SDS polyacrylamide gel and revealed by western blotting with an antibody against the hexahistidine tag.

Co-immunoprecipitation assay. *ced-5(n1812)* animals carrying two different integrated transgenes, *smIs34* (harbouring P_{ced-1}-CED-1-GFP) and *smIs118* (harbouring both P_{ttr-52}-TTR-52-Flag and P_{sur-5}-SUR-5-GFP) were used for the co-IP assay. Animals were grown in liquid culture at 20 °C for 5 days and heat shocked at 33 °C

for 45 min. After a further 6 h of growth at 20 °C, the animals were harvested and lysed as described previously⁵⁴. The supernatant was collected after centrifugation at 14,000g and 4 °C for 30 min, precleared with Protein G beads (GE Healthcare) and then incubated for 2 h with the M2 anti-Flag antibody (Sigma-Aldrich) and Protein G beads at 4 °C with gentle rocking. After four extensive washes with the same buffer, the sample was resolved on a 15% SDS polyacrylamide gel, transferred to a polyvinylidene fluoride membrane and blotted with an anti-GFP antibody (Zymed Laboratories). The same blot was then stripped of both primary and secondary antibodies in 62.5 mM Tris-HCl pH 6.8, 2% SDS, 100 mM 2-mercaptoethanol at 50 °C for 30 min, washed three times with PBST (containing 137 mM NaCl, 2.7 mM KCl, 100 mM Na₂HPO₄, 2 mM KH₂PO₄ and 0.05% Tween-20), and re-probed with an M2 anti-Flag antibody.

PtdSer binding assays. The wild-type *Saccharomyces cerevisiae* strain (BY4743; a gift from Y. Zhang, National Institute of Biological Sciences, Beijing) and the homozygous diploid knockout strain *cho1* (YSC1021-98804848, YER026C, clone ID 37756; Open Biosystems) were streaked on YPAD plates and cultured at 30 °C. The p416GPD vectors expressing GFP-Lact-C2, TTR-52-mCherry or TTR-52(M5)-mCherry were transformed into both wild-type and *cho1* yeast cells, followed by colony selection on agar plates with synthetic medium lacking uracil. A single colony was selected and cultured overnight in uracil drop-out synthetic medium at 30 °C, and the resulting yeast cells were examined with an Axioimager M1 equipped with epifluorescence. To select and culture the transformed *cho1* strain, the uracil-minus agar plates or medium were supplemented with 1 mM ethanolamine (Sigma-Aldrich). For *in vitro* PtdSer binding assay, TTR-52-mCherry-Flag and TTR-52(M5)-mCherry-Flag were affinity-purified from the medium of 293T cells transfected with pCMV-TTR-52-mCherry-Flag and pCMV-TTR-52(M5)-mCherry-Flag, respectively, and used for the *in vitro* lipid binding assay. Membrane strips spotted with various phospholipids (P-6001; Echelon Biosciences, USA) were first blocked with buffer B (25 mM Tris-HCl at pH 7.0, 150 mM NaCl, 0.1% Tween 20, 1% dried milk, 1 mM ZnSO₄, 2 mM CaCl₂) for 1 h at 22 °C and then incubated overnight at 4 °C with affinity-purified TTR-52 proteins in buffer B without dried milk. The membrane strip was washed three times in buffer B without dried milk and blotted with the M2 anti-Flag antibody.

Gonad staining by recombinant TTR-52. The *ex vivo* staining of dissected gonads by TTR-52-mCherry was performed as described previously, with some modifications¹⁹. In brief, gravid hermaphrodite adults were dissected in a gonad dissection buffer¹⁹ supplemented with 1 mM ZnSO₄, and the exposed gonads were incubated for 2 h with recombinant TTR-52 proteins in the same buffer at room temperature. The stained gonads were washed three times with the same buffer before being examined with a Nomarski microscope with epifluorescence.

Heat shock treatment. Animals at various stages were incubated at 33 °C for 1 h (+HS) or left at 20 °C without heat shock treatment (–HS), followed by recovery at 20 °C. Cell corpses and TTR-52 expression were examined 3.5 h after the heat shock treatment. Heat shock treatment did not affect the localization of TTR-52 or cell corpse engulfment in wild-type or *ced-1(e1735)* animals (Supplementary Information, Fig. S5).

Plasmid construction. Standard methods of cloning, sequencing and PCR amplification were used. We obtained full-length *ttr-52* cDNA by reverse transcription coupled with PCR (RT-PCR) using the sense primer (5'-ATGTCGAGATTTTGTGATTACTTCTCGCC-3') and the antisense primer (5'-TTAGTAGTCTTCAAGGTATCGATC-3'). To construct P_{ttr-52}-TTR-52-GFP, we first inserted a genomic fragment containing the *ttr-52* open reading frame (ORF) into the pPD95.77 vector through its *SphI* and *Sall* sites to create a TTR-52-GFP fusion, which was then PCR amplified and inserted into the heat-shock vectors pPD49.78 and pPD49.83 through their *NheI* sites. The mutated TTR-52-GFP constructs P_{ttr-52}-TTR-52(F11D, F12D)-GFP and P_{ttr-52}-TTR-52(V43M)-GFP were generated with a QuickChange mutagenesis kit (Stratagene). P_{ttr-52}-TTR-52(21–135)-GFP was constructed by amplifying the truncated TTR-52-GFP fragment from P_{ttr-52}-TTR-52-GFP and inserting it into the heat-shock vectors through their *NheI* sites. To generate P_{ttr-52}-TTR-52-mCherry, an *NheI*-*XhoI* fragment containing the full-length *ttr-52* cDNA was inserted into the heat-shock vectors along with a *Sall*-*SpeI* fragment containing the mCherry coding region as well as the 3' untranslated region of *unc-54* by a three-piece ligation method. To construct P_{ttr-52}-mCherry, a 1.3-kb DNA region

upstream of the start codon of the *ttr-52* gene was amplified by PCR and inserted into a pPD95.77-mCherry vector through its *Bam*HI and *Kpn*I sites. To construct P_{dpy-30} TTR-52, P_{egl-1} TTR-52 and P_{ced-1} TTR-52, a fragment containing the full-length *ttr-52* cDNA was inserted into the P_{dpy-30}, P_{egl-1} and P_{ced-1} vectors, respectively, through their *Nhe*I and *Nco*I sites. P_{hsp} TTR-52(M5)-mCherry were made with a QuickChange mutagenesis kit. To construct the pCMV-mCherry-Flag vector, a mCherry-Flag fragment was PCR amplified from the pPD95.75-mCherry vector and subcloned into the pCMV-Myc vector through its *Kpn*I and *Not*I sites. pCMV-TTR-52-mCherry-Flag or pCMV-TTR-52(M5)-mCherry-Flag was constructed by inserting a full-length TTR-52 or TTR-52(M5) cDNA into the pCMV-mCherry-Flag vector through its *Eco*RI and *Xho*I sites, respectively. p416GPD-GFP-Lact-C2 was constructed by amplifying the GFP-Lact-C2 fragment from the pEGFP-C1-GFP-Lact-C2 vector (Haematologic Technologies Inc.) and subcloning it into the p416GPD vector through its *Hind*III and *Xho*I sites. To generate p416GPD-TTR-52-mCherry or p416GPD-TTR-52(M5)-mCherry, TTR-52-mCherry or TTR-52(M5)-mCherry was PCR amplified and inserted into the p416GPD vector through its *Eco*RI and *Xho*I sites.

Statistical analysis. The standard error of the mean was used as *y* error bars for bar figures plotted from the mean valued of the data. Data derived from

different genetic backgrounds at multiple developmental stages were compared by two-way analysis of variance. Post hoc comparisons were done by Fisher's PLSD (protected least-squares difference). Data derived from different genetic backgrounds at a specific developmental stage were compared by Student's two-tailed unpaired *t*-test. Data were considered statistically different at $P < 0.05$. In all related panels, $P < 0.0001$ is marked with double asterisks and $P < 0.05$ is labelled with single asterisks.

Sequences. The GenBank accession numbers of *ttr-52* are HM130527 (cDNA) and HM130528 (genomic).

50. Brenner, S. The genetics of *Caenorhabditis elegans*. *Genetics* **77**, 71–94 (1974).
51. Riddle, D. L., Blumenthal, T., Meyer, B. J. & Preiss, J. R. (eds). *C. elegans II* (Cold Spring Harbor Laboratory Press, 1997).
52. Ellis, R. E., Jacobson, D. M. & Horvitz, H. R. Genes required for the engulfment of cell corpses during programmed cell death in *Caenorhabditis elegans*. *Genetics* **129**, 79–94 (1991).
53. Parrish, J. *et al.* Mitochondrial endonuclease G is important for apoptosis in *C. elegans*. *Nature* **412**, 90–94 (2001).
54. Geng, X. *et al.* Inhibition of CED-3 zymogen activation and apoptosis in *Caenorhabditis elegans* by caspase homolog CSP-3. *Nat. Struct. Mol. Biol.* **15**, 1094–1101 (2008).

DOI: 10.1038/ncb2068

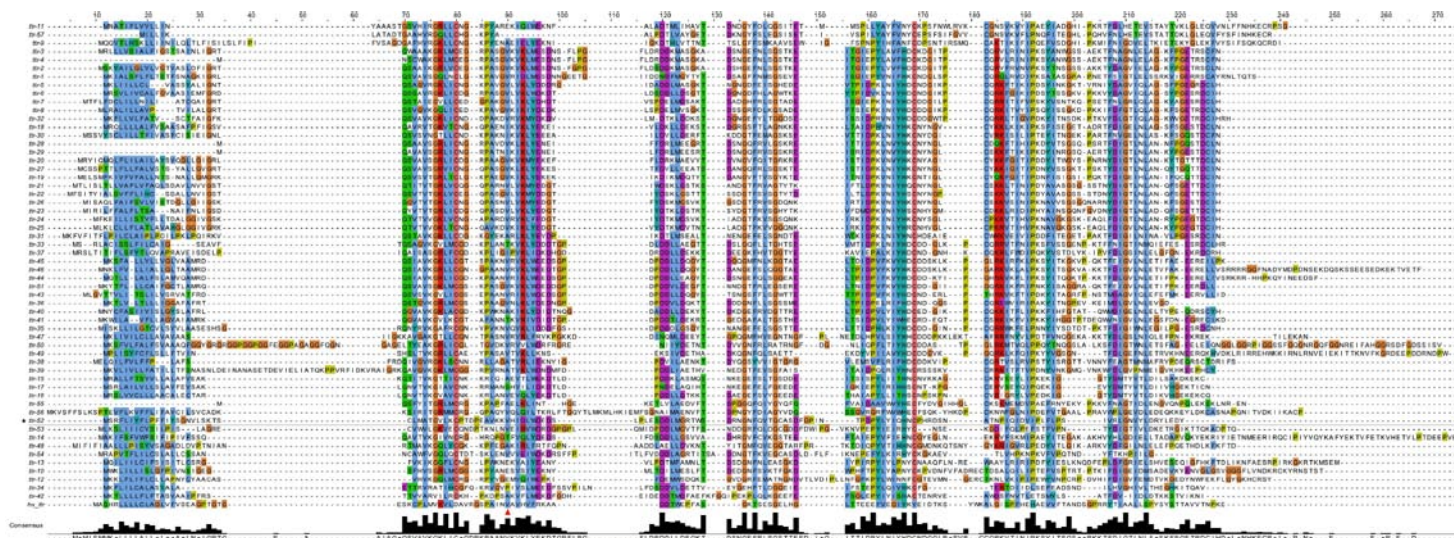


Figure S1 TTR Alignment. Amino acid sequences for *C. elegans ttr-1* through *ttr-57* and human transthyretin (*hs ttr*) were compiled and aligned using Jalview multiple alignment editor (jalview.org). Highly conserved residues are highlighted with different colors. Transthyretin-like domain is

indicated with a green bar. The valine residue mutated in the *ttr-52(sm211)* mutant is highly conserved among worm TTR proteins and human transthyretin and is indicated with a red arrowhead. The sequence of TTR-52 is underlined.

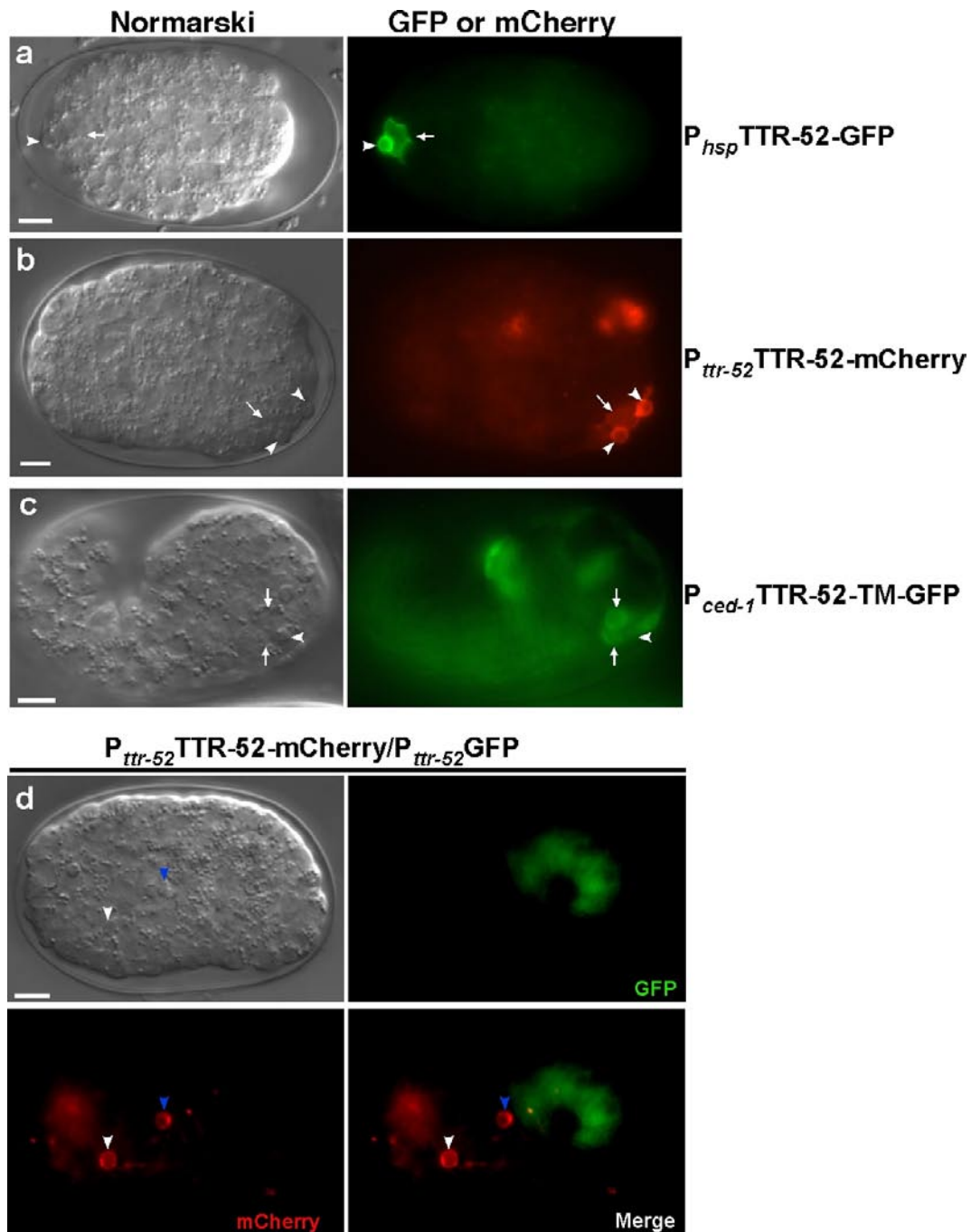


Figure S2 TTR-52 also labels the surface of living cell adjacent to the apoptotic cell and labels apoptotic cells situated far apart from where it is synthesized. **(a-b)** Nomarski and fluorescent images of a wild type *C. elegans* embryo transgenic for $P_{hsp}TTR-52-GFP$ **(a)** or $P_{ttr-52}TTR-52-mCherry$ **(b)** are shown. TTR-52 strongly labeled the surface of apoptotic cells (arrowheads), which displayed a raised disc-like morphology, and also weakly labeled the surface of living cells adjacent to the dying cells (arrows). **(c)** Membrane-tethered TTR-52-GFP failed to cluster around the apoptotic cell. Nomarski and fluorescent images of a wild-type embryo transgenic for $P_{ced-1}TTR-52-TM-GFP$ are shown. TTR-52-GFP was seen on the surface of living cells (arrows), but failed to surround an adjacent apoptotic cell

(arrowhead). **(d)** TTR-52 is synthesized in and secreted from intestine cells and labels apoptotic cells situated far apart from where it is made. Nomarski and fluorescent images of a wild-type embryo transgenic for both $P_{ttr-52}GFP$ and $P_{ttr-52}TTR-52-mCherry$ are shown. The endogenous *ttr-52* promoter (P_{ttr-52}) directs GFP expression only in intestine cells. In contrast, TTR-52-mCherry expressed under the control of the same *ttr-52* promoter was not seen in intestine cells. Instead, TTR-52-mCherry was observed outside of the intestine region and labeled strongly apoptotic cells located either close to (blue arrowhead) or far apart from intestine cells (white arrowhead), suggesting that TTR-52 is secreted and diffuses from intestine cells. Scale bars in all panels are 5 μm .

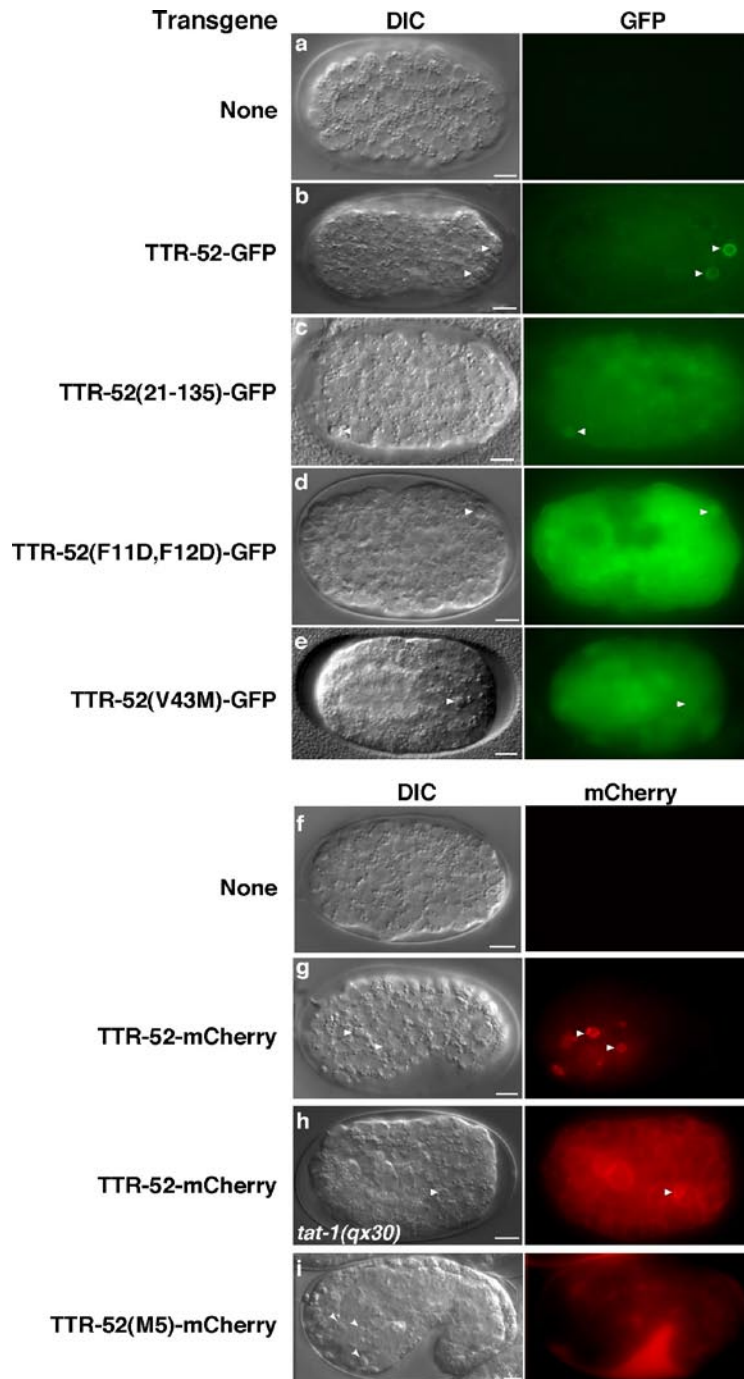


Figure S3 Expression of TTR-52 GFP or mCherry fusions in transgenic *C. elegans* embryos. Nomarski (DIC) and GFP or mCherry images of a wild-type *C. elegans* embryo transgenic for P_{hsp} TTR-52-GFP (b), P_{hsp} TTR-52(21-135)-GFP (c), P_{hsp} TTR-52(F11D, F12D)-GFP (d), P_{hsp} TTR-52(V43M)-GFP (e), P_{hsp} TTR-52-mCherry (*smls119*, g), or P_{hsp} TTR-52(M5)-mCherry (i) are shown. In h, Nomarski and mCherry images of a *tat-1(qx30)* embryo transgenic for P_{hsp} TTR-52-mCherry (*smls119*) are shown. Apoptotic cells are indicated with arrowheads. Exposure times were 3000 ms (a-e) and 500 ms (f-i), respectively. Images of non-transgenic embryos were captured through the same FITC (a) or Rhodamine channel (f). In a-e, compared with the non-transgenic embryo (a), which displayed no GFP fluorescence, TTR-

52-GFP, TTR-52(21-135)-GFP, and TTR-52(V43M)-GFP were expressed at comparable levels and TTR-52(F11D, F12D)-GFP was expressed at a higher level than the other TTR-52 GFP fusions. Similar GFP expression was observed in three independent transgenic lines for each construct. In f-i, compared with the non-transgenic embryo (f), which displayed no mCherry fluorescence, TTR-52-mCherry expression from the *smls119* integrated transgene (harboring P_{hsp} TTR-52-mCherry) in the wild-type embryo (g) was lower than its expression from the same *smls119* transgene in the *tat-1(qx30)* embryo (h) or TTR-52(M5)-mCherry expression in the wild-type embryo (i), which displayed strong mCherry fluorescence in embryo cavity. Scale bars in all panels indicate 5 μ m.

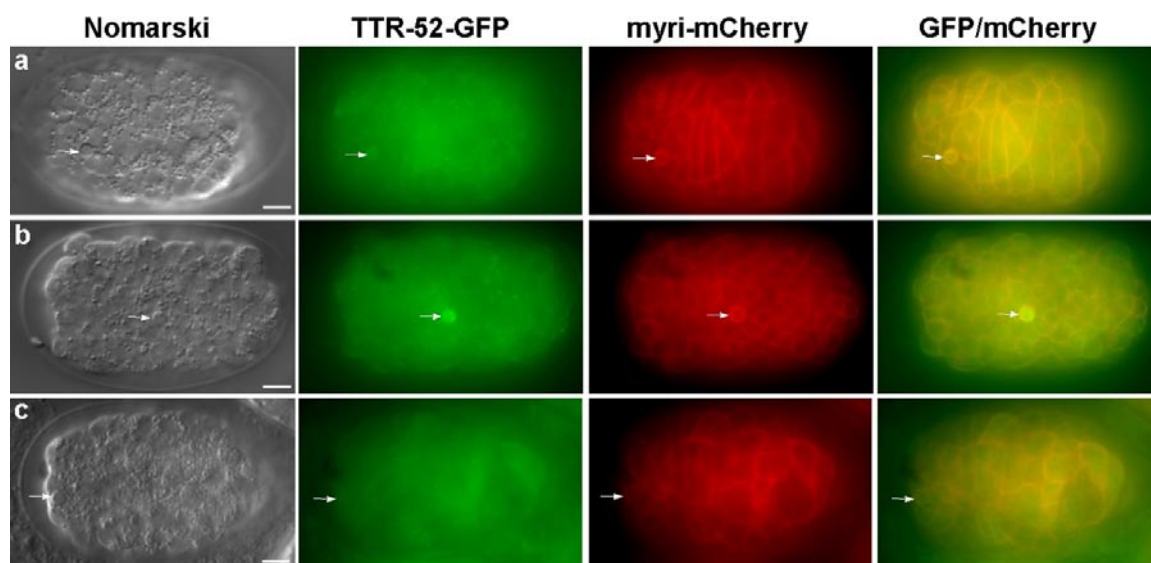


Figure S4 Various TTR-52 mutants are not secreted and appear in both cytosol and nucleus. **(a-c)** Nomarski, GFP, mCherry images and the merged images of GFP and mCherry of a wild-type embryo transgenic for P_{hsp} myri-mCherry and P_{hsp} TTR-52(21-135)-GFP **(a)**, or P_{hsp} TTR-52(F11D, F12D)-

GFP **(b)**, or P_{hsp} TTR-52(V43M)-GFP **(c)** are shown. Mutant TTR-52-GFP fusions were seen inside both apoptotic (arrows) and non-apoptotic cells, whose plasma membrane was labeled by myristoylated mCherry (myri-mCherry). Scale bars in all panels indicate 5 μ m.

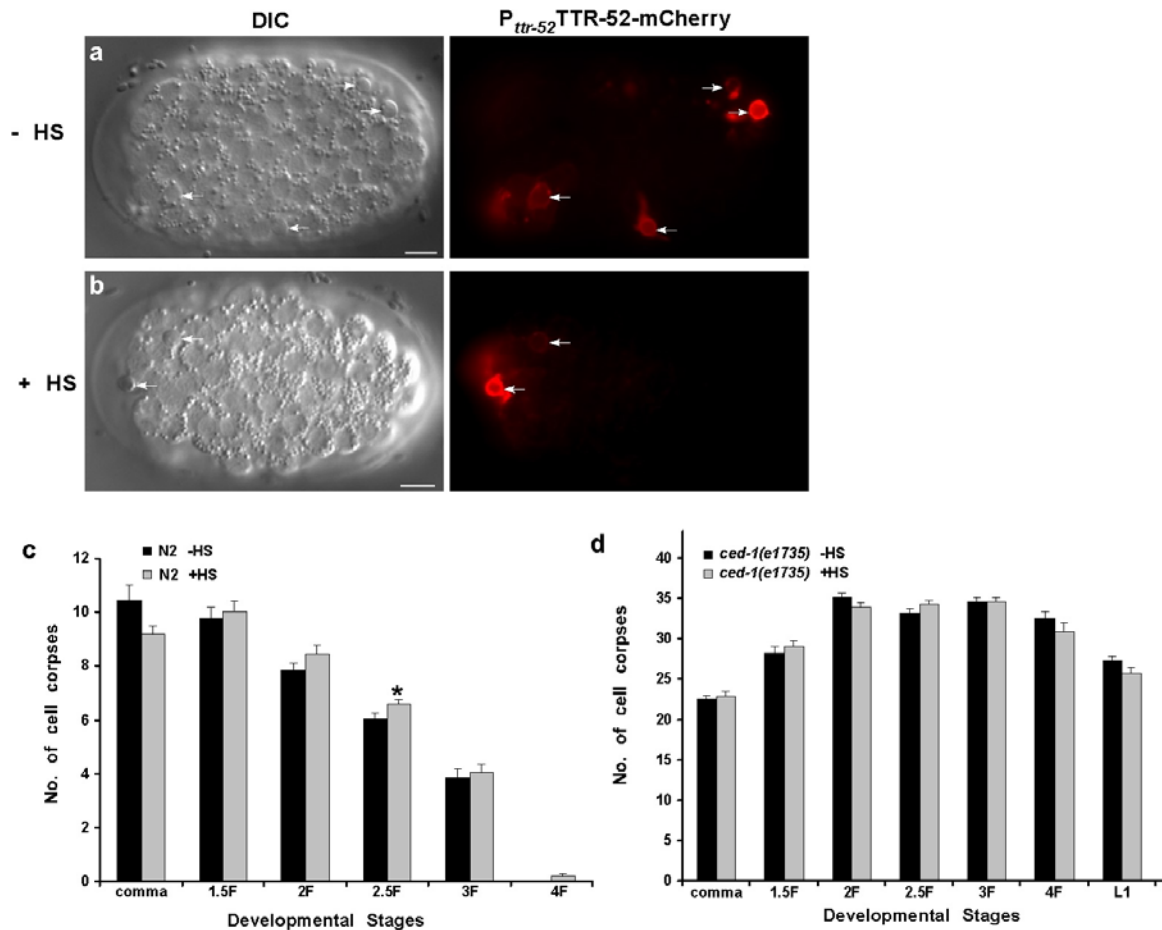


Figure S5 Heat-shock treatment does not affect TTR-52 localization and cell corpse engulfment. **(a-b)** TTR-52-mCherry expressed under the control of the *ttr-52* promoter strongly labeled the surface of apoptotic cells (arrows) with (+HS) or without (-HS) heat-shock treatment (see Methods). 20 embryos were examined for each condition. **(c-d)** Heat-shock treatment

does not affect cell corpse engulfment. Time-course analysis of embryonic and L1 larval cell corpses was performed as described in Fig. 1 in wild type **(c)** and *ced-1(e1735)* animals **(d)** with or without heat-shock treatment. 15 animals were scored for each stage. Error bars indicate SEM. Scale bars indicate 5 μ m.

Fig. 4d

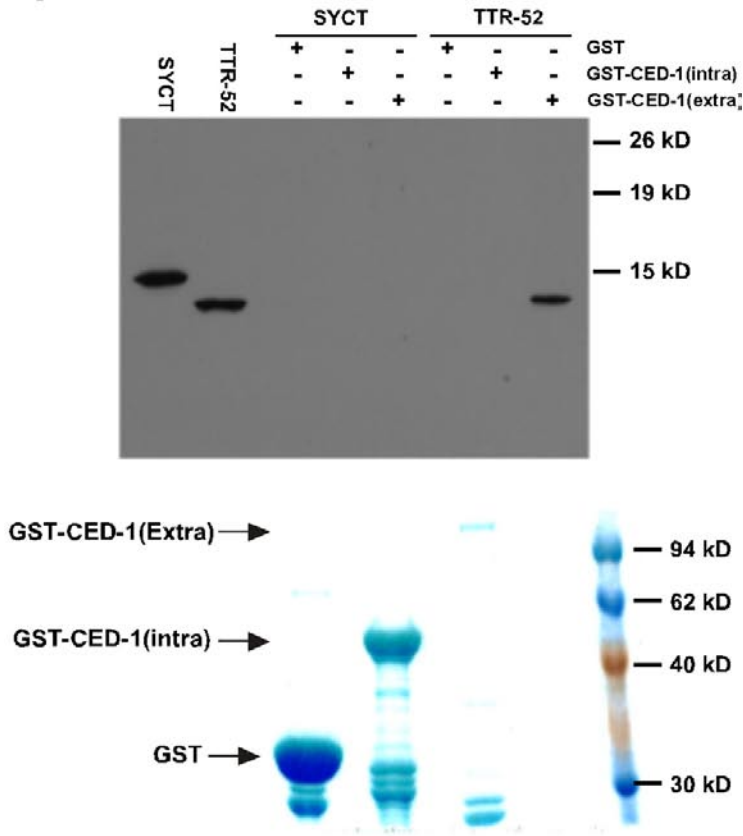


Fig. 6i

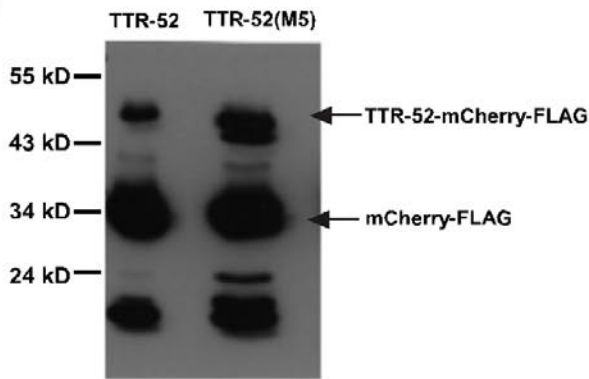


Figure S6 Full scans of immunoblots and protein gel shown in Fig. 4d and Fig. 6i.

Table S1. *ttr-52(sm211)* enhances the cell death defect of the weak *ced-3* and *ced-4* mutants

Genotype	No. extra cells	No. scored	Range
N2	0.03 ± 0.03	30	0-1
<i>ttr-52(sm211)</i>	0.5 ± 0.11	30	0-2
<i>ced-3(n2438)</i>	1.2 ± 0.22	30	0-5
<i>ttr-52(sm211); ced-3(n2438)</i>	5.6 ± 0.39	20	3-9
<i>ced-4(n2273)</i>	2.5 ± 0.19	30	1-5
<i>ttr-52(sm211); ced-4(n2273)</i>	3.7 ± 0.46	20	1-7

Extra cells were scored in the anterior pharynx of L4 hermaphrodites using Nomarski optics as described previously¹. The data shown are mean \pm S.E.M.

Table S2 A majority of the *C. elegans* transthyretin-like proteins are predicted to be secretory proteins

gene	C-score	S-score	Y-score	Secretory	gene	C-score	S-score	Y-score	Secretory
<i>ttr-1</i>	+	+	+	Yes	<i>ttr-29</i>	-	-	-	No
<i>ttr-2</i>	+	+	+	Yes	<i>ttr-30</i>	+	+	+	Yes
<i>ttr-3</i>	+	+	+	Yes	<i>ttr-31</i>	+	+	+	Yes
<i>ttr-4</i>	-	-	-	No	<i>ttr-32</i>	+	+	+	Yes
<i>ttr-5</i>	+	+	+	Yes	<i>ttr-33</i>	+	+	+	Yes
<i>ttr-6</i>	+	+	+	Yes	<i>ttr-34</i>	+	+	+	Yes
<i>ttr-7</i>	+	+	+	Yes	<i>ttr-35</i>	+	+	+	Yes
<i>ttr-8</i>	+	+	+	Yes	<i>ttr-36</i>	+	+	+	Yes
<i>ttr-9</i>	+	+	+	Yes	<i>ttr-37</i>	-	+	+	possible
<i>ttr-10</i>	+	+	+	Yes	<i>ttr-38</i>	+	+	+	Yes
<i>ttr-11</i>	+	+	+	Yes	<i>ttr-39</i>	+	+	+	Yes
<i>ttr-12</i>	+	+	+	Yes	<i>ttr-40</i>	+	+	+	Yes
<i>ttr-13</i>	+	+	+	Yes	<i>ttr-41</i>	+	+	+	Yes
<i>ttr-14</i>	+	+	+	Yes	<i>ttr-42</i>	+	+	+	Yes
<i>ttr-15</i>	+	+	+	Yes	<i>ttr-43</i>	+	+	+	Yes
<i>ttr-16</i>	+	+	+	Yes	<i>ttr-44</i>	+	+	+	Yes
<i>ttr-17</i>	+	+	+	Yes	<i>ttr-45</i>	+	+	+	Yes
<i>ttr-18</i>	+	+	+	Yes	<i>ttr-46</i>	+	+	+	Yes
<i>ttr-19</i>	+	+	+	Yes	<i>ttr-47</i>	+	+	+	Yes
<i>ttr-20</i>	+	+	+	Yes	<i>ttr-48</i>	+	+	+	Yes
<i>ttr-21</i>	+	+	+	Yes	<i>ttr-49</i>	+	+	+	Yes
<i>ttr-22</i>	+	+	+	Yes	<i>ttr-50</i>	+	+	+	Yes
<i>ttr-23</i>	+	+	+	Yes	<i>ttr-51</i>	+	+	+	Yes
<i>ttr-24</i>	+	+	+	Yes	<i>ttr-52</i>	+	+	+	Yes
<i>ttr-25</i>	+	+	+	Yes	<i>ttr-53</i>	+	+	+	Yes
<i>ttr-26</i>	+	+	+	Yes	<i>ttr-54</i>	+	+	+	Yes
<i>ttr-27</i>	+	+	+	Yes	<i>ttr-55</i>	-	-	-	No
<i>ttr-28</i>	-	-	-	No	<i>ttr-56</i>	+	+	+	Yes
					<i>ttr-57</i>	+	+	+	Yes

The blast search was carried out using SignalP 3.0 (<http://www.cbs.dtu.dk/services/SignalP/>).

C-score indicates the raw cleavage site score. S-score indicates the signal peptide score.

Y-score indicates the geometric average between the C-score and a smoothed derivative of the S-score. A protein is predicted to be a secretory protein if all three scores are positive. A protein is considered to be a non-secretory protein if all three scores are negative.

1. Ledwich, D., Wu, Y. C., Driscoll, M. & Xue, D. Analysis of programmed cell death in the nematode *Caenorhabditis elegans*. *Methods Enzymol.* 322, 76-88 (2000).